Inorganic Chemistry

Article

pubs.acs.org/IC

Speciation of the Potential Antitumor Agent Vanadocene Dichloride in the Blood Plasma and Model Systems

Daniele Sanna,[†] Valeria Ugone,[§] Giovanni Micera,[§] Tiziana Pivetta,[#] Elisa Valletta,[#] and Eugenio Garribba*[,§]

[†]Istituto CNR di Chimica Biomolecolare, Trav. La Crucca 3, I-07040 Sassari, Italy

[§]Dipartimento di Chimica e Farmacia and Centro Interdisciplinare per lo Sviluppo della Ricerca Biotecnologica e per lo Studio della Biodiversità della Sardegna, Università di Sassari, Via Vienna 2, I-07100 Sassari, Italy

[#]Dipartimento di Scienze Chimiche e Geologiche, Università di Cagliari, Cittadella Universitaria, I-09042 Monserrato, Cagliari, Italy

Supporting Information

ABSTRACT: The speciation of the potential antitumor agent vanadocene dichloride ($[Cp_2VCl_2]$, abbreviated with VDC) in the blood plasma was studied by instrumental (EPR, ESI-MS, MS-MS, and electronic absorption spectroscopy) and computational (DFT) methods. The behavior of VDC at pH 7.4 in aqueous solution, the interaction with the most important bioligands of the plasma (oxalate, carbonate, phosphate, lactate, citrate, histidine, and glycine among those with low molecular mass and transferrin and albumin between the proteins) was evaluated. The results suggest that $[Cp_2VCl_2]$ transforms at physiological pH to $[Cp_2V(OH)_2]$ and that only oxalate, carbonate, phosphate, and lactate are able to displace the two OH^- ions to yield $[Cp_2V(ox)]$, $[Cp_2V(CO_3)]$, $[Cp_2V(lactH_{-1})]$, and $[Cp_2V(HPO_4)]$. The formation of the adducts with oxalate, carbonate, lactate, and hydrogen phosphate was confirmed also by ESI-MS and MS-MS spectra. The stability order is $[Cp_2V(ox)] \gg [Cp_2V(CO_3)] > [Cp_2V(lactH_{-1})] > [Cp_2V(HPO_4)]$. No interaction between VDC and plasma proteins was detected under our experimental conditions. Several model systems containing the bioligands (bL) in the same relative ratio as in the blood samples were also examined. Finally, the speciation of VDC in the plasma was studied. The results obtained show that the model systems behave as the blood plasma and indicate that when V concentration is low (10 μM) VDC is transported in the bloodstream as $[Cp_2V(ox)]$; when V concentration is high (100 μM) oxalate binds only 9.2 μM of $[Cp_2V]^{2+}$, whereas the remaining part distributes between $[Cp_2V(CO_3)]$ (main species) and $[Cp_2V(lactH_{-1})]$ (minor species); and when V concentration is in the range 10−100 μM $[Cp_2V]^{2+}$ distributes between $[Cp_2V(ox)]$ and $[Cp_2V(CO_3)]$.

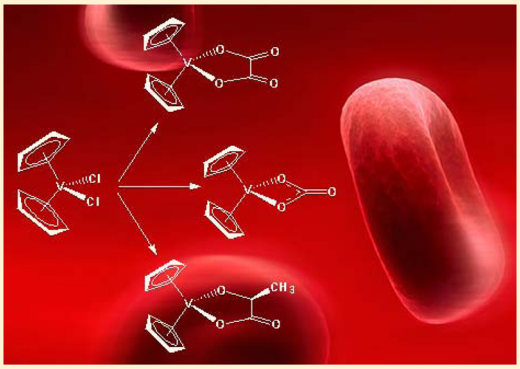

INTRODUCTION

Vanadium plays a number of roles in biological systems and has been found in many naturally occurring compounds.[1] In humans, vanadium compounds exhibit a wide variety of pharmacological properties. In particular, the antidiabetic activity has been extensively studied during the last 20 years;[2] bis(maltolato)oxidovanadium(IV) (or BMOV) became the benchmark complex for the new molecules with antidiabetic action,[3] and its derivative bis(ethylmaltolato)oxidovanadium(IV) (or BEOV) arrived to phase IIa of the clinical trials,[4] even if these have provisionally been abandoned due to renal problems arising with several patients.[5,6] Furthermore, vanadium complexes have been tested as antiparasitic, spermicidal, antiviral, anti-HIV, and antituberculosis agents.[5,7]

The first report on the potential anticancer action of a vanadium compound, bis(cyclopentadienyl)vanadium(IV) dichloride or vanadocene dichloride ($[Cp_2VCl_2]$ abbreviated to VDC, Scheme 1a), active in the treatment of Ehrlich ascites tumor, dates back to 1983.[8] Subsequently, VDC underwent the same extensive preclinical testing against both animal and human cell lines alongside the parent compound $[Cp_2TiCl_2]$ (TDC).[9] The clinical test on TDC stopped at phase II of the clinical trials, due to the low efficacy in patients with metastatic renal cell carcinoma or metastatic breast cancer.[10] However, in all the studies in vitro $[Cp_2VCl_2]$ was found to be more active than $[Cp_2TiCl_2]$; in particular, in a systematic study on the activity of several metallocenes on the human testicular cancer cell lines Tera-2 and Ntera-2, only vanadocene derivatives exhibited significant cytotoxicity leading the tumor cells to apoptosis within 24 h.[9a] A very active derivative of VDC is bis[(*p*-methoxybenzyl)cyclopentadienyl]vanadium(IV) dichloride (vanadocene **Y**, Scheme 1b), which exhibits an IC_{50} value of 3.0 μM against the LLC-PK (pig kidney epithelial) cell line (in contrast, the value of titanocene **Y** is significantly higher, 21 μM).[11] This is a particularly encouraging datum, since

Received: March 18, 2015
Published: August 17, 2015

DOI: 10.1021/acs.inorgchem.5b01277
Inorg. Chem. 2015, 54, 8237−8250

Scheme 1. Structure of Vanadocene Dichloride (VDC) (a) and Its Derivatives Vanadocene Y (b) and Diisoselenocyanate Vanadocene Y (c)

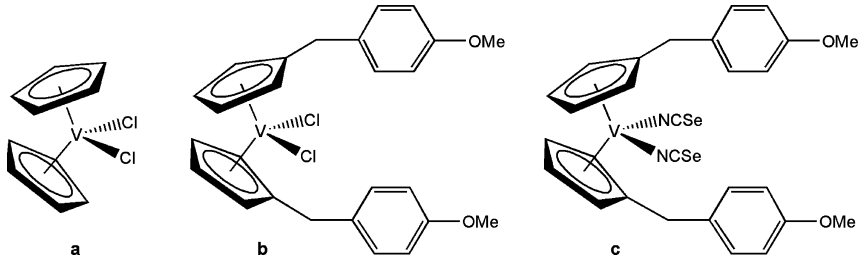

vanadocene **Y** is slightly more active against this cell line than the "classic" cisplatin, which shows an IC_{50} value of 3.3 μM.[11] Recently, in vitro experiments on modified vanadocene **Y** (diisoselenocyanate vanadocene **Y**, Scheme 1c) have shown impressive cytotoxic effects against the human renal cancer cells CAKI-1, with an IC_{50} value reaching for the first time the nanomolar range for metallocene anticancer potential drugs.[12] A comprehensive study of the cytotoxic activity of methyl- and methoxy-substituted VDC toward T-lymphocytic leukemia cells MOLT-4 has been recently reported.[13] Under the physiological conditions, the $[Cp_2V]^{2+}$ moiety remains essentially intact, while the auxiliary X ligand, chloride or isoselenocyanate, is subject to substitution by H_2O/OH^- that can further be exchanged for functions provided by DNA. However, in contrast with Pt(II), V(IV) is a particularly hard metal center and thus should preferentially bind to phosphate residues of DNA rather than N bases of guanosine.[7a]

The speciation of an active metal complex in the blood is an important aspect of the drug metabolism, and the form transported to the target organs significantly affects its efficiency and mechanism of action. The assumption that the V complexes (and metal complexes, in general) reach the target cells in the same form as they are administrated can be considered an oversimplification.[14] Indeed, in the blood ligand exchange and complexation reactions by the components of the plasma are possible; moreover, a V compound can distribute between plasma and erythrocytes.[15] All of the main proteins of the plasma, such as transferrin (hTf), albumin (HSA), and immunoglobulin G (IgG), and the low molecular mass (*l.m.m.*) bioligands, such as oxalate, lactate, phosphate, citrate, and amino acids, can interact with the V compound administered and partly or fully displace the organic ligands.[16,17] For example, it has been recently demonstrated through an X-ray determination that lysozyme replaces the water molecule equatorially coordinated in the insulin-mimetic agent $[VO(pic)_2(H_2O)]$ through the COO^- group of the Asp-52 residue.[18] Unfortunately, the study of the speciation of a metal complex in a complicated system such as the blood plasma is not an easy task because plasma contains many bioligands with very different concentration and molecular mass[19] and many chemical reactions—as mentioned above—are possible. For this reason, in many cases model systems have been investigated to infer indirect information on the biological system.[20] However, very often the results obtained in the models are not fully in agreement with those observed in the real systems and give only partial information.

In this work, the speciation of VDC in several model systems and in blood plasma was studied and compared. It has been noted recently that the paramagnetic nature of the V(IV) center (electronic configuration $3d^1$), which precludes the use of classical NMR tools, makes the characterization of these complexes and their biologically active species more difficult than the parent titanocene derivatives, and this slowed down their analysis and the advances in this topic.[21] However, EPR spectroscopy is a valid tool to characterize V(IV) in solution;[22] for example, nonoxido V(IV) complexes display distinctive spectroscopic features, in particular, hyperfine coupling constants *A* much smaller than those observed for V(IV)O species.[23] Herein, EPR characterization was supported by electronic absorption spectroscopy[24] and electrospray ionization mass spectrometry (ESI-MS), which allows the detection of metal complexes and adducts that readily fragment.[25,26] Tandem mass spectrometry (MS-MS) was used to confirm the stoichiometry of the species. Computational methods based on DFT (density functional theory) provide other valuable information on the coordination mode of the bioligands on and the environment of V(IV) species.[27]

The results reported in this study on the model systems perfectly coincide with those observed in a complex real system such as the plasma and allow the prediction of the speciation of VDC in the blood as a function of the vanadium concentration in the organism.

EXPERIMENTAL AND COMPUTATIONAL SECTION

Chemicals. Water was deionized prior to use through the purification system Millipore Milli-Q Academic. Vanadocene dichloride was a Sigma-Aldrich product. 4-(2-Hydroxyethyl)-1-piperazineethanesulfonic acid (HEPES), sodium hydrogen carbonate ($NaHCO_3$), sodium hydrogen phosphate (Na_2HPO_4), citric acid (H_3citr), lactic acid (Hlact), oxalic acid (H_2ox), histidine (His), and glycine (Gly) were Sigma-Aldrich, Merck, or Carlo Erba products of the highest grade available and used as received. Human serum apotransferrin (98%, T4283) and human serum albumin (97−99%, A9511) were purchased from Sigma-Aldrich with a molecular mass of 76−81 and 66 kDa, respectively.

Methanol (CH_3OH) for LC-MS and trifluoroacetic acid (TFA) used in the ESI-MS and MS-MS experiments were purchased from Sigma-Aldrich.

Preparation of the Solutions for Spectroscopic Measurements. The solutions were prepared by dissolving in ultrapure water, obtained through the purification system Millipore Milli-Q Academic, weighted amounts of VDC and bioligands.

In the binary systems VDC concentration was 1.0×10^{-3} M, and the VDC to bioligand ($NaHCO_3$, Na_2HPO_4, oxalic acid, lactic acid, citric acid, histidine, glycine) molar ratio was 1/10 (Figures S5−S9 of Supporting Information). In all systems the pH was adjusted to 7.4, and spectra were immediately recorded. Argon was bubbled through the solutions during their preparation to ensure the absence of oxygen and avoid oxidation of the V(IV) ion. The eventual oxidation of V(IV) to V(V), therefore, could start only during the spectroscopic measurements.

In the multicomponent systems containing VDC and the bioligands ($NaHCO_3$, Na_2HPO_4, oxalic acid, lactic acid) three types of

DOI: 10.1021/acs.inorgchem.5b01277
Inorg. Chem. 2015, 54, 8237−8250

experiments were carried out: (i) in the first experiment the VDC and bioligands concentration was 1.0×10^{-3} M and 1.0×10^{-2} M and the molar ratio VDC/bL was 1/10 (Figures 3 and S11 and S12 of the Supporting Information); (ii) in the second one VDC concentration was 4.0×10^{-4} M and the ratio VDC/ox/$NaHCO_3$/lact/Na_2HPO_4 1/1/2706.5/164.1/119.6 (Figures 4–6); (iii) in the third one VDC concentration was 4.0×10^{-4} M and the ratio VDC/ox/$NaHCO_3$/lact/Na_2HPO_4 1/0.1/270.7/16.4/12.0 (Figures 5, 7, and S13 of the Supporting Information). In all experiments the pH was brought to 7.4 and argon was bubbled through the solutions to avoid oxidation of the V(IV) ion.

EPR spectra with the physiological concentrations of the bioligands (and metal ion) cannot be measured because very low intensity signals would be detected. To overcome this problem we used higher concentrations of the metal ion (4.0×10^{-4} M) and bioligands but maintaining the same ratio as in a blood plasma. The same strategy was previously used when studying the distribution of insulin-enhancing $V(IV)O^{2+}$ complexes between the high and low molecular mass components of the plasma, with the extrapolation to low concentrations being a normal procedure used in the literature.[17c,20,28,29]

In the experiments involving apo-hTf a concentration of VDC of 5.0×10^{-4} M was used. The pH was raised to ca. 4.0, and $NaHCO_3$ and HEPES were added in appropriate amounts in order to have a concentration of 2.5×10^{-2} and 1.0×10^{-1} M, respectively. Subsequently, pH was brought to ca. 5.0, and apo-hTf was added to the solution to obtain a final concentration of 2.5×10^{-4} M. Finally, pH was increased to 7.40. In the experiments involving HSA the concentration of VDC was 1.0×10^{-3} M. The pH was raised to ca. 5.0, and HEPES and HSA were added to have a concentration of 1.0×10^{-1} and 2.5×10^{-4} M. Then the pH was brought to 7.40. In all systems, the spectra were immediately measured to minimize the possible oxidation of V(IV) to V(V).

Experiments with Blood Plasma. Blood samples were obtained from Servizio Trasfusionale Aziendale (ASL of Sassari). Blood samples were centrifuged for 10 min at 3000 rpm, and the plasma was separated from buffy coat and red blood cells. The plasma was subsequently incubated for 30 min at 37 °C with a solution of VDC to have a final concentration of 4.5×10^{-5} M. The EPR spectrum was immediately measured.

Spectroscopic Measurements. EPR spectra were recorded at room temperature (298 K) or on frozen solutions (120 K) using an X-band (9.4 GHz) Bruker EMX spectrometer equipped with an HP 53150A microwave frequency counter. When the signal-to-noise ratio was low due to the low V(IV) concentration, signal averaging was used.[30] Electronic absorption spectra were obtained with a PerkinElmer Lambda 35 spectrophotometer.

Mass Spectrometry. The aqueous sample solutions containing VDC or the adducts with oxalate, lactate, carbonate, and hydrogen phosphate were prepared in ultrapure water obtained with Milli-Q Millipore. To improve the quality of the spectra, all solutions were mixed in a 1:1 v/v ratio with methanol containing 1% of TFA. These solutions were infused in the ESI chamber immediately after their preparation in order not to modify the aqueous solution equilibria. Mass spectra in positive- and negative-ion mode were obtained on a triple-quadrupole QqQ Varian 310-MS mass spectrometer using the atmospheric-pressure technique. The sample solutions were infused into the ESI source using a programmable syringe pump at a flow rate of 1.00 mL/h. A dwell time of 14 s was used, and the spectra were accumulated for at least 10 min in order to increase the signal-to-noise ratio. Mass spectra were recorded in the m/z range 50–500 at a final concentration of 5.0×10^{-4} M. The experimental conditions used for the measurements were: needle voltage 4500 V, shield voltage 600 V, housing temperature 60 °C, drying gas temperature 100 °C, nebulizer gas pressure 40 PSI, drying gas pressure 20 PSI, and detector voltage 1450 V. MS-MS experiments were performed with argon as collision gas (1.8 PSI) using a needle voltage of 6000 V, shield voltage of 800 V, housing temperature of 60 °C, drying gas temperature of 120 °C, nebulizer gas pressure of 40 PSI, drying gas pressure of 20 PSI, and detector voltage of 2000 V. Collision energy was varied from 2 to 50 eV. The isotopic patterns of the experimental peaks were analyzed using the mMass 5.5.0 software package.[31]

DFT Calculations. DFT (density functional theory) calculations were performed with the software Gaussian 03 (revision C.01)[32] and ORCA.[33]

The geometry of V(IV) complexes was optimized with Gaussian at the B3P86/6-311g level of theory with the procedure reported in the literature.[34] This choice ensures a good degree of accuracy in the prediction of the structures of first-row transition metal complexes[35] and, in particular, of vanadium species.[34] For all structures, minima were verified through frequency calculations.

On the optimized structures, the ^{51}V hyperfine coupling tensor $\boldsymbol{A}$ was calculated with Gaussian software using the hybrid functional half-and-half BHandHLYP and the basis set 6-311g(d,p) and with ORCA software using the hybrid functional PBE0 and the basis set VTZ, according to the procedures previously published.[36] It must be taken into account that for a V(IV) species A is usually negative, but in the literature its absolute value is often reported; this formalism was also used in a number of points of this study. The ^{51}V $\boldsymbol{A}$ tensor has three contributions: the isotropic Fermi contact (A^{FC}), the anisotropic or dipolar hyperfine interaction ($\boldsymbol{A}^{D}$), and one second-order term that arises from spin–orbit (SO) coupling ($\boldsymbol{A}^{SO}$):[33b] $\boldsymbol{A} = A^{FC}\mathbf{1} + \boldsymbol{A}^{D} + \boldsymbol{A}^{SO}$, where $\mathbf{1}$ is the unit tensor. The values of the ^{51}V anisotropic hyperfine coupling constants along the x, y, and z axes are as follows: $A_x = A^{FC} + A_x^{D} + A_x^{SO}$, $A_y = A^{FC} + A_y^{D} + A_y^{SO}$, and $A_z = A^{FC} + A_z^{D} + A_z^{SO}$. From these equations, the value of A_{iso} is $A_{iso} = (1/3)(A_x + A_y + A_z) = A^{FC} + (1/3)(A_x^{SO} + A_y^{SO} + A_z^{SO}) = A^{FC} + A^{PC}$, where the term $(1/3)(A_x^{SO} + A_y^{SO} + A_z^{SO})$ is named isotropic pseudocontact, A^{PC}.[33b] Gaussian neglects the second-order term represented by $\boldsymbol{A}^{SO}$; thus, $A^{PC} = 0$ and $A_{iso} = A^{FC}$. The theory background was described in detail in ref 37. The percent deviation from the experimental value $|A_i|^{exptl}$, where i = iso, x, y, was calculated as $100 \times [(|A_i|^{calcd} - |A_i|^{exptl})/|A_i|^{exptl}]$.

RESULTS AND DISCUSSION

1. Behavior of VDC in Aqueous Solution. The behavior of VDC in aqueous solution has been investigated through the combined application of EPR, UV–vis spectroscopy, ESI-MS, MS-MS, and DFT methods. The structure of VDC has been already solved by X-ray diffraction analysis:[38] it is tetrahedral with two sites occupied by the cyclopentadienyl rings and the other two sites by the ions Cl^-. The geometry of VDC has been optimized with Gaussian 03 software through DFT methods, which give good results in the optimization of the structure of transition metal complexes[35] and of vanadium complexes in particular.[34] The structure of VDC is shown in Figure S1a of the Supporting Information, and a comparison between the bond distances and angles is given in Table S1.

The behavior of $[Cp_2VCl_2]$ in aqueous solution has been examined by Toney and Marks and, subsequently, by Pavlík and Vinklárek.[39–41] The results indicate that the two Cp–V bonds are more resistant to hydrolysis than the analogous compounds of titanium and zirconium, $[Cp_2TiCl_2]$ and $[Cp_2ZrCl_2]$, and the stability order is V > Ti > Zr. When $[Cp_2MCl_2]$ (M = V, Ti, Zr) are dissolved in water the dissociation of both the Cl^- ions is revealed, with the dissociation of the first chloride being too fast to be observed and the half-life time for the dissociation of the second one being 50 (M = Ti), 30 (M = Zr), and 24 min (M = V). The dissociation constant for the loss of the first Cl^- is very large and cannot be measured; that for the second Cl^- is 4.2×10^{-2} (M = Ti) and 2.7×10^{-3} M (M = V).[40] In the system with VDC, the species formed at acid pH is $[Cp_2V(H_2O)_2]^{2+}$, whose structure has been determined by X-ray diffraction analysis[39] and simulated in this study (Table S1 and Figure S1b of the Supporting Information). The two water molecules bound to vanadium(IV) in $[Cp_2V(H_2O)_2]^{2+}$ are strongly acid (pK_a =

DOI: 10.1021/acs.inorgchem.5b01277
Inorg. Chem. 2015, 54, 8237–8250

4.73 and 5.15).[40] Pavlík and Vinklárek demonstrated that $[Cp_2V(H_2O)_2]^{2+}$ is stable in aqueous solution for several days. They also proved that at pH 7.4 the only species present in solution is $[Cp_2V(OH)_2]$, whose EPR signal disappears after exposition to air for 72 h.[41]

The behavior of VDC in aqueous solution has been re-examined in this work through EPR and UV−vis spectroscopy and the ESI-MS technique as the basis for the study of its speciation in the blood plasma under the physiological pH. EPR spectra recorded as a function of pH on a solution containing VDC 1.0×10^{-3} M (Figure S2 of Supporting Information) show, according to the results reported in the literature, the presence of $[Cp_2V(H_2O)_2]^{2+}$ in acid solution (pH < 4.0) and of $[Cp_2V(OH)_2]$ in neutral and basic solution (pH > 6.0). The intermediate species $[Cp_2V(H_2O)(OH)]^+$ is not observable because the two deprotonations of the water molecules overlap for the very close values of pK_a.[40] Room-temperature EPR spectra are characterized by a significant variation of g_{iso} and A_{iso} from $[Cp_2V(H_2O)_2]^{2+}$ (g_{iso} = 1.980 and $A_{iso} = 73.5 \times 10^{-4}$ cm^{-1}) to $[Cp_2V(OH)_2]$ (g_{iso} = 1.985 and $A_{iso} = 58.4 \times 10^{-4}$ cm^{-1}), see Figure S3 of the Supporting Information.

The mass spectrum of VDC (Figure 1) shows, in particular, the peaks of $[Cp_2VCl]^+$ (m/z 216) and $[Cp_2V(OH)]^+$ (m/z 198). Other peaks were also identified, such as those of $[Cp_2V(TFA)]^+$ (m/z 294), $[Cp_2VF]^+$ (m/z 200), $[2Cp+3H]^+$ (m/z 133), and $[Cp_2V]^{2+}$ (m/z 90), but they were recognized as products of the fragmentation−recombination reactions occurring in ESI phase. All identified signals are listed in Table 4, together with the fragmentation products of the most intense peaks. Calculated and experimental isotopic patterns for selected peaks are reported in Figure S4 of the Supporting Information. The stoichiometry of the hypothesized species was confirmed by MS-MS experiments.

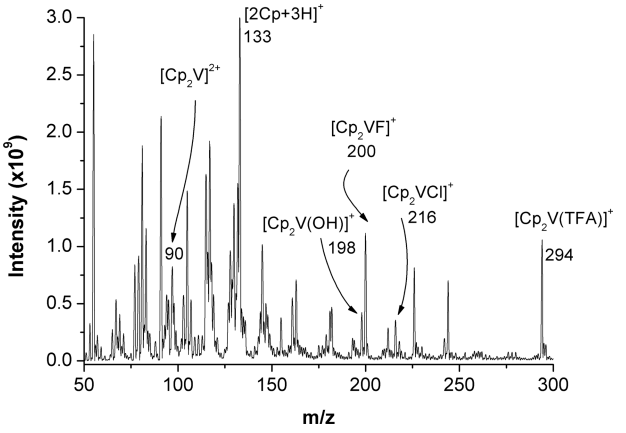

Figure 1. Positive ESI mass spectrum of VDC (5.0×10^{-4} M), recorded in H_2O/CH_3OH 1:1 v/v (1% TFA).

The A_{iso} values were calculated by DFT methods, which are a good tool to predict the hyperfine coupling constants between the unpaired electron with ^{51}V nucleus measured in an EPR spectrum.[42,43] According to the procedures established in the literature,[37c] the calculations were performed with Gaussian 03 (which does not include the spin−orbit coupling) using the half-and-half functional BHandHLYP and the basis set 6-311g(d,p) and ORCA (which takes into account the second-order spin−orbit contribution) with the functional PBE0 and the basis set VTZ. To the best of our knowledge, no systematic study on the prediction of the EPR parameters (tensors $\boldsymbol{g}$ and $\boldsymbol{A}$) for nonoxido vanadium(IV) complexes was published, but recent results indicate that ORCA performs slightly better than Gaussian because the percent contribution of the spin−orbit coupling to A_{iso} is larger than in the case of $V(IV)O^{2+}$ complexes,[44] i.e., the pseudocontact term $A^{PC} = (1/3)(A_x^{SO} + A_y^{SO} + A_z^{SO})$ is not negligible with respect to Fermi contact, A^{FC} (see Experimental and Computational Section). The results obtained for VDC and the V(IV) species formed in solution, including those with the bioligands, are listed in Table 1.

From the data reported in Table 1, it emerges that ORCA performs better than Gaussian in the prediction of A_{iso}. This difference can be attributed to the term A^{PC} (considered by ORCA and not by Gaussian), which contributes for 8−10% to A_{iso}. On the basis of the results, it can be argued that a DFT calculation with ORCA can be used to predict the A_{iso} value of a V(IV) complex; in particular, a calculation performed at the level of theory PBE0/VTZ allows one to predict A_{iso} with a mean deviation from the experimental value of 3.1% (Table 1).

2. Interaction of VDC with the l.m.m. Bioligands of the Blood Serum. Among the low molecular mass bioligands of the blood serum (bL), oxalate (ox), lactate (lact), citrate (citr), hydrogen phosphate (HPO_4^{2-}), glycine (Gly), histidine (His), and carbonate (CO_3^{2-}) are the most likely potential V(IV) binders.[16a,20] In this work, the systems VDC/bL were studied at the physiological pH using a ratio of 1/10 and VDC

Table 1. Experimental (exptl) and Calculated (calcd) Isotropic Hyperfine Coupling Constants (A_{iso}) for VDC, Its Hydrolytic Products, and Ternary Complexes[a]

	exptl		calcd (Gaussian)[b]		calcd (ORCA)[c]	
complex	g_{iso}	A_{iso}	A_{iso}	dev. %[d]	A_{iso}	dev. %[d]
$[Cp_2VCl_2]$	1.978	−69.1	−59.6	−13.7	−64.0	−7.4
$[Cp_2V(H_2O)_2]^{2+}$	1.980	−73.5	−71.6	−2.6	−78.3	6.5
$[Cp_2V(OH)_2]$	1.985	−58.4	−52.6	−9.9	−60.0	2.7
$[Cp_2V(ox)]$	1.983	−63.5	−56.1	−11.7	−63.8	0.5
$[Cp_2V(CO_3)]$	1.985	−58.3	−51.8	−11.1	−59.6	2.2
$[Cp_2V(lactH_{-1})]$	1.984	−63.6	−58.1	−8.6	−65.7	1.7
$[Cp_2V(citrH_{-1})]^{3-}$	1.987	−65.4	−62.8	−4.0	−67.2	2.8
$[Cp_2V(HPO_4)]$	1.993	−63.3	−55.9	−11.7	−63.4	0.2
MAD[e]				9.5		3.1

[a] A_{iso} value measured in 10^{-4} cm^{-1}. [b] Values calculated at the level of theory BHandHLYP/6-311g(d,p). [c] Values calculated at the level of theory PBE0/VTZ. [d] Percent deviation from the experimental value, $|A_{iso}|^{exptl}$, calculated as $100 \times [(|A_{iso}|^{calcd} - |A_{iso}|^{exptl})/|A_{iso}|^{exptl}]$. [e] Mean of the absolute percent deviations (MAD) from the experimental values.

DOI: 10.1021/acs.inorgchem.5b01277
Inorg. Chem. 2015, 54, 8237−8250

Scheme 2. Structures of $[Cp_2V(ox)]$ (a), $[Cp_2V(lactH_{-1})]$ (b), $[Cp_2V(CO_3)]$ (c), and $[Cp_2V(HPO_4)]$ (d)

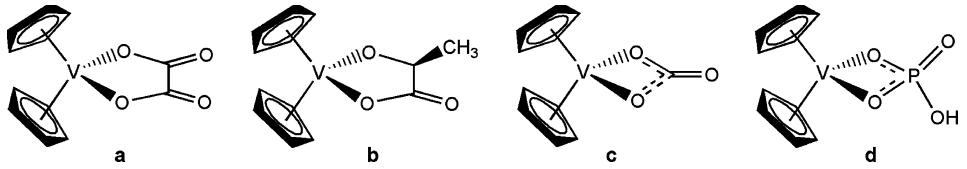

Table 2. Experimental (exptl) and Calculated (calcd) Anisotropic Hyperfine Coupling Constants (A_i) for Ternary Complexes Formed by VDC[a]

	calcd (Gaussian)[b]			calcd (ORCA)[c]			exptl[d]		% (Gaussian)		% (ORCA)	
	A_x	A_y	A_z	A_x	A_y	A_z	A_x	A_y	% $\lvert A_x\rvert$[e]	% $\lvert A_y\rvert$[e]	% $\lvert A_x\rvert$[e]	% $\lvert A_y\rvert$[e]
$[Cp_2V(ox)]$	−91.7	−74.9	−1.6	−98.4	−85.4	−7.5	−102.1	−77.9	−10.2	−3.9	−3.7	9.7
$[Cp_2V(CO_3)]$	−87.9	−70.8	3.3	−95.5	−79.9	−3.3	−94.5	−75.9	−7.0	−6.7	1.0	5.3
$[Cp_2V(lactH_{-1})]$	−94.9	−78.7	−0.7	−101.9	−88.0	−7.2	−101.7	−79.1	−6.7	−0.5	0.2	11.3
MAD[f]									8.0	3.7	1.6	8.8

[a]All values measured in 10^{-4} cm^{-1}. [b]Values calculated at the level of theory BHandHLYP/6-311g(d,p). [c]Values calculated at the level of theory PBE0/VTZ. [d]A_z not measurable. [e]Percent deviation from the experimental value, $\lvert A_i\rvert^{exptl}$ (i = x, y), calculated as $100 \times [(\lvert A_i\rvert^{calcd} - \lvert A_i\rvert^{exptl})/\lvert A_i\rvert^{exptl}]$. [f]Mean of the absolute percent deviations (MAD) from the experimental values.

Scheme 3. Possible Coordination Modes of Hydrogen Phosphate (a−c) and (bi)Carbonate (d−f) to the $[Cp_2V]^{2+}$ Moiety of VDC

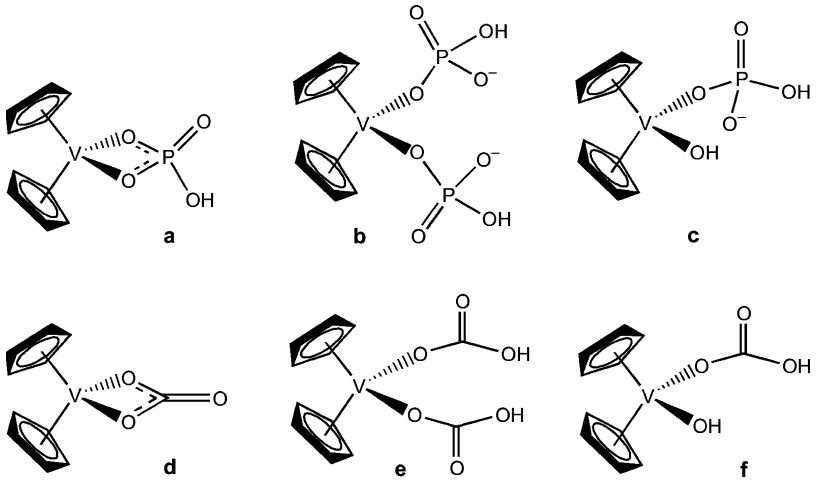

concentration of 1×10^{-3} M. EPR and UV−vis spectra were compared with those of $[Cp_2V(OH)_2]$, which—as mentioned above—is the only species existing at pH 7.4 when VDC is dissolved in aqueous solution. ESI-MS, MS-MS spectra, and DFT calculations were carried out to confirm the results (see below). The oxidation of V(IV) to V(V) is negligible at the experimental conditions used in this study, and EPR and UV−vis data support this conclusion: indeed, the spectroscopic signals of the main V(IV) species existing at pH 7.4 do not change significantly as a function of time.

The formation of the ternary species in the solid state between the moiety $[Cp_2V]^{2+}$ and mono- and bidentate ligands was demonstrated in the literature. In particular, Vinklárek and co-workers prepared solid samples upon reaction of VDC with amino acids with noncoordinating[45] and coordinating side-chain groups,[46] with phosphate,[47] oxalate,[48] and carbonate.[49] The results of the spectroscopic measurements revealed in this study on the systems VDC/oxalate, VDC/lactate, VDC/citrate, VDC/HCO_3^-, VDC/HPO_4^{2-}, VDC/Gly, and VDC/His showed that only oxalate, lactate, carbonate, and hydrogen phosphate are able to replace the two OH^- ions of $[Cp_2V(OH)_2]$ to yield mixed species (Figure S5 of Supporting Information). Glycine and histidine, in contrast with what was observed in the solid state, do not form ternary complexes in solution, whereas in the system with citrate the amount of mixed compound is significantly lower than that of $[Cp_2V(OH)_2]$ (Figure S6 of the Supporting Information).

In the system with oxalate, the formation of a neutral species $[Cp_2V(ox)]$ was detected. Oxalate binds vanadium(IV) with the two oxygen atoms of carboxylate groups forming a five-membered chelate ring (Scheme 2a). The concentration of this species is close to 100% (Figure S5, trace b). The structural details calculated by DFT methods for the species $[Cp_2V(ox)]$ are compared with those determined in the solid state through X-ray diffraction analysis by Honzíček et al. (Table S2 of the Supporting Information).[48] Another aspect to be noticed is the small line width of the eight resonances ($\Delta H_1 = 6.5 \times 10^{-1}$ mT and $\Delta H_8 = 9.3 \times 10^{-1}$ mT); here, we would like to stress that this observation will be very important when the distribution of $[Cp_2V]^{2+}$ between the bioligands of the blood serum will be discussed. The formation of $[Cp_2V(ox)]$ from $[Cp_2V(OH)_2]$ is also demonstrated by examination of the electronic absorption spectra reported in Figure S7 of the Supporting Information (traces black and red).

DOI: 10.1021/acs.inorgchem.5b01277
Inorg. Chem. 2015, 54, 8237−8250

Table 3. Experimental (exptl) and Calculated (calcd) Isotropic Hyperfine Coupling Constants (A_{iso}) with the Nuclei of ^{51}V, ^{31}P, and ^{13}C for the Possible Ternary Complexes Formed by VDC with HPO_4^{2-} and CO_3^{2-} Anions[a]

	A_{iso} (^{51}V)[b]		A_{iso} (^{31}P)[c]		A_{iso} (^{13}C)[d]	
species	calcd (Gaussian)	calcd (ORCA)	calcd (Gaussian)	calcd (ORCA)	calcd (Gaussian)	calcd (ORCA)
$[Cp_2V(HPO_4)]$	−55.9	−63.4	33.2	45.3		
$[Cp_2V(HPO_4)_2]^{2-}$	−56.6	−64.7	1.5	2.6		
$[Cp_2V(HPO_4)(OH)]^-$	−55.7	−64.1	4.9	5.7		
$[Cp_2V(CO_3)]$	−51.8	−59.6			10.5	17.4
$[Cp_2V(HCO_3)_2]$	−64.3	−70.6			1.7	6.1
$[Cp_2V(HCO_3)(OH)]$	−60.6	−66.3			1.1	3.5

[a]All values measured in 10^{-4} cm^{-1}. [b]The experimental value of A_{iso} (^{51}V) for the ternary complex formed in the system VDC/HPO_4^{2-} is -63.3×10^{-4} cm^{-1}, while that for the ternary complex formed in the system VDC/HCO_3^- is -58.3×10^{-4} cm^{-1}. [c]The experimental value of A_{iso} (^{31}P) for the ternary complex formed in the system VDC/HPO_4^{2-} is 27.5×10^{-4} cm^{-1} (ref 47). [d]The experimental value of A_{iso} (^{13}C) for the ternary complex formed in the system VDC/HCO_3^- is 8.0×10^{-4} cm^{-1} (ref 49).

The frozen solution EPR spectrum of $[Cp_2V(ox)]$ is reported in trace a of Figure S8 of Supporting Information, whereas the values of A_x, A_y, and A_z calculated with Gaussian and ORCA are listed in Table 2. Also, in the case of the anisotropic hyperfine constants, the prediction of ORCA is slightly better than that of Gaussian.

To the best of our knowledge, the system VDC/lactate was never studied up to now. The room-temperature EPR spectrum recorded at pH 7.4 is shown in Figure S5, trace a, and the frozen solution spectrum in Figure S8, trace b. The spectroscopic data (Tables 1 and 2) show that a mixed species with composition $[Cp_2V(lactH_{-1})]$ is formed (the structure is represented Scheme 2b), in which lactate binds V(IV) with the donor set (COO^-, O^-). This species is present in solution with a small amount of the bis-chelated $V(IV)O^{2+}$ complex, $[VO(lactH_{-1})_2]^{2-}$, in which lactate in the doubly deprotonated form binds vanadium with the coordination mode 2 × (COO^-, O^-).[50] The line width of the eight resonances of the room-temperature spectrum ($\Delta H_1 = 8.1 \times 10^{-1}$ mT and $\Delta H_8 = 12.0 \times 10^{-1}$ mT) is larger than that of the analogous species of oxalate, $[Cp_2V(ox)]$. The electronic absorption spectrum of $[Cp_2V(lactH_{-1})]$ (Figure S7, green) differs significantly from that of $[Cp_2V(OH)_2]$ (Figure S7, black).

The room-temperature EPR spectrum recorded at the physiological pH in the system with hydrogen phosphate is reported in Figure S5, trace c. It is possible to observe that instead of the eight transitions expected for a mononuclear V(IV) species, 16 resonances are revealed. This is due to the coupling of the unpaired electron with the nucleus of ^{31}P (I = 1/2) and is in agreement with the results in the literature.[47] Concerning the species formed under these experimental conditions, three possibilities for coordination of the HPO_4^{2-} ion must be taken into account: in the first it is bidentate and forms a four-membered chelated cycle (Scheme 3a), in the second one it is monodentate and replaces only one OH^- ion (Scheme 3b), and in the third one two HPO_4^{2-} anions replace both OH^- ligands in $[Cp_2V(OH)_2]$ (Scheme 3c).

Some years ago, Vinklárek and co-workers demonstrated through the combined application of spectroscopic and computational methods that $[Cp_2V(HPO_4)]$ exists in solution.[47] Here, we repeated the DFT calculations: the values of A_{iso} for the coupling between the unpaired electron and the nuclei of ^{51}V and ^{31}P were calculated with the software Gaussian and ORCA for $[Cp_2V(HPO_4)]$, $[Cp_2V(HPO_4)_2]^{2-}$, and $[Cp_2V(HPO_4)(OH)]^-$ and are reported in Table 3. In agreement with the results reported,[47] the best agreement with the experimental data is obtained for $[Cp_2V(HPO_4)]$ with a bidentate coordination mode of hydrogen phosphate (Scheme 3a). In particular, the high value of A_{iso} (^{31}P) is compatible only with this species. The electronic spectrum of $[Cp_2V(HPO_4)]$ is represented in Figure S7, purple, and is different from those of the other mixed complexes and of $[Cp_2V(OH)_2]$.

In the system with the ion HCO_3^- the formation of only one species is observed in the room-temperature spectrum (Figure S5, trace d) with g_{iso} = 1.985 and $A_{iso} = 58.3 \times 10^{-4}$ cm^{-1}. These parameters are very similar to those of $[Cp_2V(OH)_2]$, in agreement with what is predicted by DFT calculations (Table 1). The anisotropic EPR spectrum recorded at 120 K in the system VDC/HCO_3^- at pH 7.4 with a ratio 1/10 is shown in Figure S9, trace b, and is compared with that expected for $[Cp_2V(CO_3)]$ on the basis of the calculations with ORCA software. From an examination of Figure S9, it can be observed that the agreement between the two spectra is rather good. The formation of $[Cp_2V(CO_3)]$ was demonstrated in the literature by Vinklárek et al.[45,49] Another confirmation of the formation of $[Cp_2V(CO_3)]$ is the significant difference in the electronic absorption spectra recorded at pH 7.4 in the systems containing only VDC and VDC/HCO_3^- (cfr. traces black and blue in Figure S7).

As for hydrogen phosphate, carbonate could bind to the unit $[Cp_2V]^{2+}$ in three different modes represented in Scheme 3d–f. In this case too, the comparison between the experimental values of A_{iso} (^{51}V) and A_{iso} (^{13}C) allowed us to demonstrate that the correct coordination mode for CO_3^{2-} ligand is the bidentate one. For example, the values of A_{iso} (^{51}V) predicted for structures d, e, and f of Scheme 3 are 59.6, 70.6, and 66.3 × 10^{-4} cm^{-1} (with ORCA), respectively, to be compared with 58.3×10^{-4} cm^{-1} experimentally measured. These results are in agreement with those obtained by Vinklárek and co-workers.[45,49]

The formation of the mixed species revealed by EPR and UV–vis spectroscopy and DFT calculations was confirmed by ESI-MS and MS-MS spectrometry preparing solutions containing VDC and the bioligand in 1/1–1/10 ratios. These two techniques are suitable tools for the study of metal complexes in solution.[25] Of course, in the transfer from solution to gas phase, two important phenomena may happen: (i) the redox reactions occurring at the capillary may alter the valence state of the metal ion inducing a coordination change and a structural rearrangement; (ii) the fragmentation products may themselves recombine forming new species. The mass spectra of solutions containing VDC and oxalate, lactate, or carbonate show the peaks of the corresponding adducts, i.e., $[Cp_2V(ox)+H]^+$ (m/z 270), $[Cp_2V(lactH_{-1})+H]^+$ (m/z 270),

DOI: 10.1021/acs.inorgchem.5b01277
Inorg. Chem. 2015, 54, 8237–8250

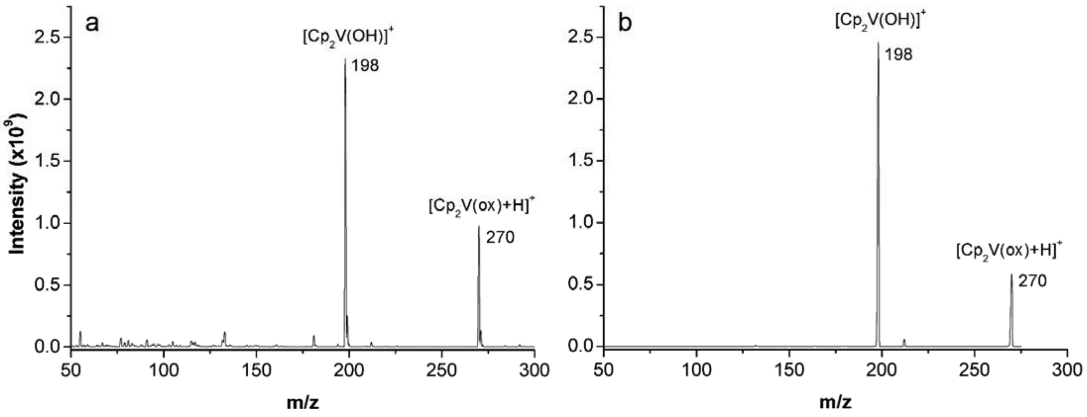

Figure 2. (a) Positive ESI mass and (b) tandem MS-MS spectrum of the solution containing VDC and oxalate (5.0×10^{-4} M, 1/1 molar ratio), recorded in H_2O/CH_3OH 1:1 v/v (1% TFA).

and $[Cp_2V(CO_3)+H]^+$ (m/z 242). In Figure 2a, the mass spectrum of the system VDC/oxalate is reported as an example. In the case of phosphate, due to the suppression effect of this ion,[51] a reliable spectrum was obtained only working with high voltages at needle (6000 V) and shield (800 V). At these conditions, a peak attributable to $[Cp_2V^V(PO_4)+Na]^+$ was found (m/z 299), together with peaks indicating the formation of polynuclear species. However, some of the detected species could have been formed in ESI phase for the severe experimental conditions used and then do not reflect the composition of the solution.

The stoichiometry hypothesized for the adducts formed with oxalate, lactate, and carbonate was confirmed by MS-MS experiments. The fragmentation profile obtained for the peak at m/z 270 for the system VDC/oxalate is reported in Figure 2b as an example. As it can be seen, the MS-MS is identical to the ESI-MS spectrum, indicating that the species with stoichiometry $[Cp_2V(OH)]^+$ (m/z 198) is a recombined fragment of the parent compound $[Cp_2V(ox)+H]^+$ (m/z 270). Therefore, the results confirm that $[Cp_2V(ox)]$ is the predominant species in solution. Analogous results were obtained in the systems with lactate and carbonate. The comparison between the calculated and the experimental isotopic pattern for $[Cp_2V(ox)+H]^+$, $[Cp_2V(lactH_{-1})+H]^+$, and $[Cp_2V^V(PO_4)+Na]^+$ is shown in Figure S4 of the Supporting Information. In Table 4 the experimental and calculated m/z values for the detected species are reported.

In contrast with the ligands discussed above, in the system with citrate $[Cp_2V(citrH_{-1})]^{2-}$ is a minor species (Figure S6 of Supporting Information, trace c). The major complex is $[Cp_2V(OH)_2]$, whereas the resonances of two $V(IV)O^{2+}$ species, $[VO(H_2O)_5]^{2+}$ (g_{iso} = 1.968 and A_{iso} = 106.9 × 10^{-4} cm^{-1}) and $[VO(citrH_{-1})]^{2-}$ (g_{iso} = 1.970 and A_{iso} = 98.0 × 10^{-4} cm^{-1}), in which citrate in the fully deprotonated form binds vanadium with the donor set (COO^-, O^-), are also detected.[50a,52]

Among the amino acids of the blood serum, in this study glycine (as an example of an amino acid without coordinating side-chain group) and histidine (as an example of an amino acid with coordinating side-chain group) were examined. The team of Vinklárek synthesized several complexes in the solid state formed by amino acids (a.a.) with structure $[Cp_2V(a.a.)]^+$.[45] When such species are dissolved in an organic solvent such as MeOH, the resonances of $[Cp_2V(a.a.)]^+$ can be revealed. The data obtained in this study indicate that the behavior in aqueous solution is different. In the system with glycine (Figure S6 of the Supporting Information, trace b) the only species is $[Cp_2V(OH)_2]$; the value of A_{iso} measured (58.3×10^{-4} cm^{-1}) is significantly different from that of the species formed by the amino acids, $[Cp_2V(a.a.)]^+$ ($62.2–62.9 \times 10^{-4}$ cm^{-1} [45]), and

Table 4. Species Identified from the ESI-MS Studies and MS-MS Fragmentation Products

	ion	composition	exptl m/z[a]	calcd m/z[a]
I	$[Cp_2V]^{2+}$ (originated from **XI** and **XIII**)	$C_{10}H_{10}V$	90.90	90.51
II	$[C_5H_6 + C_3H_3]^+$ (originated from **XIV**)	C_8H_9	104.92	105.07
III	$[CpV]^+$ (originated from **VIII** and **XVI**)	C_5H_5V	115.85	115.98
IV	$[2Cp + 3H]^+$ (originated from **IX**, **XIV** and **XVIII**)	$C_{10}H_{13}$	132.90	133.10
V	$[CpV^{III}F]^+$ (originated from **X**)	C_5H_5FV	134.91	134.98
VI	$[CpVN_2]^+$ (originated from **VIII**)	$C_5H_5N_2V$	143.87	143.98
VII	$[Cp_2V^{III}]^+$ (originated from **XI**, **XV** and **XVI**)	$C_{10}H_{10}V$	180.95	181.02
VIII	$[Cp_2VH]^+$ (MS-MS fragments: m/z 144, 116)	$C_{10}H_{11}V$	181.98	182.01
IX	$[Cp_2V(OH)]^+$ (MS-MS fragment: m/z 133)	$C_{10}H_{11}OV$	197.94	198.00
X	$[Cp_2VF]^+$ (MS-MS fragment: m/z 135)	$C_{10}H_{10}FV$	199.97	200.00
XI	$[Cp_2VCl]^+$ (MS-MS fragments: m/z 181, very low, 91)	$C_{10}H_{10}ClV$	215.98	216.00
XII	$[Cp_2V(OH)N_2]^+$ (originated from **XIV**)	$C_{10}H_{11}N_2OV$	225.94	226.03
XIII	$[Cp_2V(CO_3)+H]^+$ (MS-MS fragments: m/z 198, 91)	$C_{11}H_{11}O_3V$	242.03	242.00
XIV	$[Cp_2V(OH)(H_2O)N_2]^+$ (MS-MS fragments: m/z 226, 133, 105)	$C_{10}H_{13}N_2O_2V$	243.98	244.03
XV	$[Cp_2V(lactH_{-1})+H]^+$ (MS-MS fragments: m/z 198, 181)	$C_{13}H_{15}O_3V$	269.99	270.00
XVI	$[Cp_2V(ox)+H]^+$ (MS-MS fragments: m/z 198, 181, 116)	$C_{12}H_{11}O_4V$	270.01	270.00
XVII	$[Cp_2V(TFA)]^+$	$C_{12}H_{10}F_3O_2V$	294.04	294.00
XVIII	$[Cp_2V^V(PO_4)+Na]^+$ (MS-MS fragment: m/z 133)	$C_{10}H_{10}NaO_4PV$	299.00	299.00

[a]The experimental and calculated m/z values refer to the peak representative of the monoisotopic mass.

DOI: 10.1021/acs.inorgchem.5b01277
Inorg. Chem. 2015, 54, 8237–8250

that calculated with ORCA for $[Cp_2V(Gly)]^+$ (62.8×10^{-4} cm^{-1}). In the system with histidine the major species is $[Cp_2V(OH)_2]$, whereas the resonances of $[Cp_2V(His)]^+$ (g_{iso} = 1.984 and $A_{iso} = 62.4 \times 10^{-4}$ cm^{-1}) are much less intense, suggesting that the mixed complex is present at the physiological pH in a very low amount. Therefore, at the experimental conditions of this study, it can be affirmed that the affinity of the amino acids for the moiety $[Cp_2V]^{2+}$ is much lower than that of other *l.m.m.* bL. This may be due to the low affinity of $[Cp_2V]^{2+}$ for the nitrogen with respect to that for the oxygen donors. A demonstration of this finding is the behavior of 1-methylimidazole (that has been used over the last years by our team as a model for the coordination of an imidazole nitrogen of a histidine residue to the insulin-mimetic $V(IV)O^{2+}$ complexes[16b−i]), which does not form mixed complexes and confirms the poor affinity of $[Cp_2V]^{2+}$ ion toward the nitrogen donors.

3. Interaction of VDC with Blood Serum Proteins. The interaction of the insulin-mimetic $V(IV)O^{2+}$ complexes with the blood serum proteins has been widely studied by our team.[16b−i] The results demonstrated that both hTf and HSA bind vanadium(IV) complexes with a nitrogen donor of an accessible histidine residue, probably exposed on the protein surface. Recently, it was proved that also carboxylate of an aspartate residue is able to coordinate $V(IV)O^{2+}$ ion.[18] Some years ago, the interaction of VDC with apo-transferrin (apo-hTf) has been studied through the combined application of EPR, electronic absorption, CD, and fluorescence spectroscopy.[53,54] In particular, Nishida et al. in the system VDC/apo-hTf observed two sets of isotropic resonances with g_{iso} = 1.985 and $A_{iso} = 95.9 \times 10^{-4}$ cm^{-1} (species a) and g_{iso} = 1.984 and $A_{iso} = 58.0 \times 10^{-4}$ cm^{-1} (species b). These two signals were incorrectly attributed to the species in which $V(IV)O^{2+}$ ion is bound to the Fe sites in the *N*- and *C*-terminal regions of the protein and to the species derived from VDC in which the two Cl^- ions are replaced by O and N donors of the side chains of transferrin.[54] It is well known that EPR spectra recorded at room temperature in the systems containing proteins can be characterized by two types of signals: isotropic signals belonging to species in which V(IV) is bound to the *l.m.m.* ligands and anisotropic signals for the binary or ternary species in which V(IV) is bound to the proteins.[16f,17d,28,55] The detection of anisotropic signals at room temperature is due to slow tumbling motion, in the time scale of an EPR experiment, of the complexes formed by the proteins which behave as a solid or a frozen solution. In contrast, the signals revealed by Nishida et al. are completely isotropic, and this induces us to believe that apo-transferrin did not interact with VDC under their experimental conditions. On the basis of the results discussed above, species b observed by Nishida et al. is the complex in which two OH^- ions bind $[Cp_2V]^{2+}$ forming $[Cp_2V(OH)_2]$ ($A_{iso} = 58.0 \times 10^{-4}$ cm^{-1}), whereas species a is, without any doubt for the large value of A_{iso} (95.9×10^{-4} cm^{-1}), a $V(IV)O^{2+}$ complex; in addition, the intensity of the signal of $[Cp_2V(OH)_2]$ decreases as a function of the time and that of $V(IV)O^{2+}$ species increases significantly, indicating a V(IV)−V(IV)O transformation. Du et al., instead, proposed that the interaction between $[Cp_2VCl_2]$ and apo-hTf is similar to $[Cp_2TiCl_2]$,[53] which loses the two cyclopentadienyl rings forming Ti_2(apo-hTf);[56] this result appears to be in contrast with the fact that the fragment $[Cp_2V]^{2+}$ is much more stable than $[Cp_2Ti]^{2+}$ and that EPR data do not show the formation of $(VO)_2$(apo-hTf), whose spectrum is well known.[17b,30,55,57,58]

In this study, the system VDC/apo-hTf has been re-examined and the EPR spectrum recorded at pH 7.4 is shown in Figure S10 of the Supporting Information, trace b. Our data are in agreement with those of Nishida et al., even if the interpretation of the data is different; in particular, it emerges that the spectrum at the physiological conditions is superimposable with that of $[Cp_2V(OH)_2]$ (see traces a and b of Figure S10).

Nishida et al. also examined the system VDC/HSA. EPR signals at room temperature are isotropic with g_{iso} = 1.984 and $A_{iso} = 58.0 \times 10^{-4}$ cm^{-1}.[54] On the basis of this result, the authors concluded that albumin interacts with $[Cp_2V]^{2+}$ through surface sites of the protein, analogously to what was observed for TDC.[59] Our data confirm what was detected by Nishida et al.,[54] but in this case too the detection of isotropic signals (Figure S10 of Supporting Information, trace c) allowed us to rule out that the albumin interacts with $[Cp_2V]^{2+}$ ion. The eight resonances (which do not change as a function of the time) and the spectral parameters (g_{iso} = 1.985 and $A_{iso} = 58.3 \times 10^{-4}$ cm^{-1}) can be attributed to $[Cp_2V(OH)_2]$ (spectrum shown in trace a of Figure S10 of Supporting Information). Moreover, in both systems with apo-hTf and HSA no decrease of the isotropic signals, attributable to an interaction with the proteins such as to broaden the resonances, is observed.

In conclusion it can be argued that, under the experimental conditions used in this study, the blood plasma proteins do not interact with VDC. At the moment the reasons of this behavior are not known, but it can be hypothesized that several factors contribute to disfavor the formation of the possible ternary species formed upon interaction of the moiety $[Cp_2V]^{2+}$ with the proteins: (i) as mentioned above, the affinity of $[Cp_2V]^{2+}$ toward the nitrogen donors is rather poor, and this would preclude the bonding with His-N, which instead appears to be very important for the insulin-mimetic $V(IV)O^{2+}$ complexes;[16b−i] (ii) the protein surface is rich of polar residues such as aspartate, glutamate, tyrosine, and threonine, and this could hinder their interaction with the $[Cp_2V]^{2+}$ moiety, in which the two cyclopentadienyl rings are strongly apolar; (iii) as noticed for citrate, the presence of the two bulky cyclopentadienyls may hinder the interaction with the side chains of the amino acids of apo-hTf and HSA.

4. Speciation of VDC in Blood Plasma Model Solutions. After the examination of the binary systems formed by VDC and the main blood plasma components (bL and proteins), in this section the behavior of several model systems of the blood plasma will be discussed. In particular, the multicomponent system formed by VDC and the bioligands with higher affinity for $[Cp_2V]^{2+}$ (i.e., oxalate, carbonate, lactate, and hydrogen phosphate, see above) was studied. For all systems, room-temperature and frozen solution EPR spectra and electronic absorption spectra were recorded at pH 7.4. Initially, the molar ratio between VDC and the bioligands bL was set at 1/10, whereas subsequently it was brought to the physiological value using the relative concentration of oxalate, carbonate, lactate, and hydrogen phosphate in the plasma as reported by Harris ([ox] = 9.2 μM, $[HCO_3^-]$ = 24.9 mM, [lact] = 1.51 mM, $[HPO_4^{2-}]$ = 1.10 mM);[19] in particular, the ratios $[HPO_4^{2-}]/[ox]$, $[lact]/[ox]$, and $[HCO_3^-]/[ox]$ were 119.6, 164.1, and 2706.5, respectively.

The room-temperature EPR spectrum recorded at pH 7.4 in the system VDC/ox/$NaHCO_3$/lact with molar ratio 1/10/10/10 is shown in Figure 3b. It can be noticed that in the quaternary system the main species is $[Cp_2V(ox)]$ and

DOI: 10.1021/acs.inorgchem.5b01277
Inorg. Chem. 2015, 54, 8237−8250

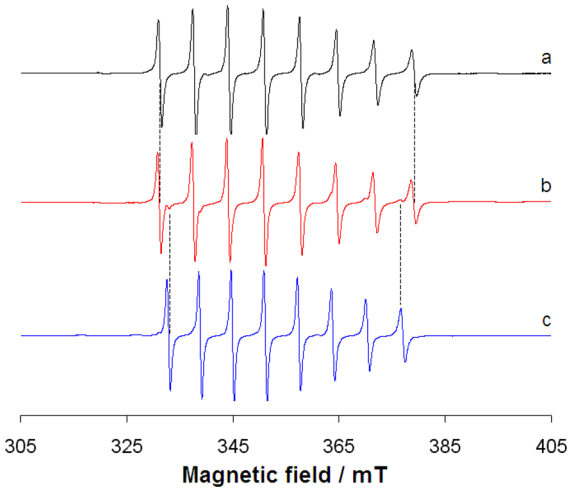

Figure 3. Room-temperature (298 K) EPR spectra recorded at pH 7.4 in aqueous solution in the systems containing (a) VDC/ox 1/10, (b) VDC/ox/$NaHCO_3$/lact 1/10/10/10, and (c) VDC/$NaHCO_3$ 1/10. VDC concentration was 1.0×10^{-3} M. With the dotted lines the resonances $M_I = -7/2, 7/2$ of the complexes $[Cp_2V(ox)]$ (trace a) and $[Cp_2V(CO_3)]$ (trace c) are shown.

$[Cp_2V(CO_3)]$ is a minor species. Even if $[Cp_2V(ox)]$ and $[Cp_2V(lactH_{-1})]$ are characterized by similar EPR parameters, the signals can be attributed without ambiguity to $[Cp_2V(ox)]$ for the small experimental line width ($\Delta H_1 = 6.2 \times 10^{-1}$ mT and $\Delta H_8 = 9.0 \times 10^{-1}$ mT, to be compared with $\Delta H_1 = 6.5 \times 10^{-1}$ mT and $\Delta H_8 = 9.3 \times 10^{-1}$ mT for $[Cp_2V(ox)]$ and $\Delta H_1 = 8.1 \times 10^{-1}$ mT and $\Delta H_8 = 12.0 \times 10^{-1}$ mT for $[Cp_2V(lactH_{-1})]$, see above). This result suggests that the affinity of $[Cp_2V]^{2+}$ for oxalate is much higher than that for carbonate and lactate.

In Figure S11 of the Supporting Information (trace b) the room-temperature EPR spectrum of the system VDC/$NaHCO_3$/lact/Na_2HPO_4 with ratio 1/10/10/10 and VDC concentration 1.0×10^{-3} M is reported. In this system the two species $[Cp_2V(CO_3)]$ (spectrum shown in trace a) and $[Cp_2V(lactH_{-1})]$ (spectrum in trace c) are formed in comparable amounts, with the concentration of the mixed complex with carbonate slightly larger than that with lactate. The possible formation of $[Cp_2V(HPO_4)]$ can be excluded because this species would be countersigned by the characteristic coupling between the unpaired electron and the ^{31}P nucleus (Figure S5, trace c).

The behavior of the ternary system VDC/lact/Na_2HPO_4 with molar ratio 1/10/10 is represented in Figure S12 of the Supporting Information (trace b). In such a system $[Cp_2V(lactH_{-1})]$ is the main species, and $[Cp_2V(HPO_4)]$ (which can be distinguished very well for the 16-line spectrum) is the minor species. This indicates that the affinity of lactate for $[Cp_2V]^{2+}$ ion is slightly higher than that of phosphate.

On the basis of these results, it can be affirmed that the affinity order of the four blood plasma bL ligands for the moiety $[Cp_2V]^{2+}$ is $ox^{2-} \gg CO_3^{2-} > lactH_{-1}^{2-} > HPO_4^{2-}$.

The systems discussed above (see Figure 3 and Figures S11 and S12 of Supporting Information), even if they allow us to demonstrate the relative strength of the bL bioligands for $[Cp_2V]^{2+}$, are not good models of the blood plasma because the relative concentrations of bL must be considered; for example, the higher affinity of oxalate may be compensated by the larger concentration of the other three components. To throw light on this point, the quinary system VDC/ox/$NaHCO_3$/lact/Na_2HPO_4 has been studied at pH 7.4 with the bioligands at the same concentration ratio as in the blood plasma. Concerning the concentration of VDC in the blood necessary to display a pharmacological effect, no decisive datum was published in the literature, but it seems to be reasonable assume that, analogously to what was reported for the insulin-mimetic vanadium compounds, the value must be in the range 10−100 μM.[1b,60] Therefore, the system VDC/ox/$NaHCO_3$/lact/Na_2HPO_4 was examined at molar ratio 1/1/2706.5/164.1/119.6 and 1/0.1/270.7/16.4/12.0 with a concentration of VDC of 4×10^{-4} M. The first model system "simulates" the situation in which the concentration in the plasma of the containing-V drug is close to that of oxalate (9.2 μM[19]), whereas in the second system the concentration is 10 times that of oxalate (92.0 μM). With this approach, the concentration range 9.2−92.0 μM of the pharmacologically active VDC can be explored.

The room-temperature spectrum recorded on the system VDC/ox/$NaHCO_3$/lact/Na_2HPO_4 with molar ratio 1/1/2706.5/164.1/119.6 is shown in Figure 4b. It can be observed that the main species is $[Cp_2V(ox)]$ (Figure 4a), whereas

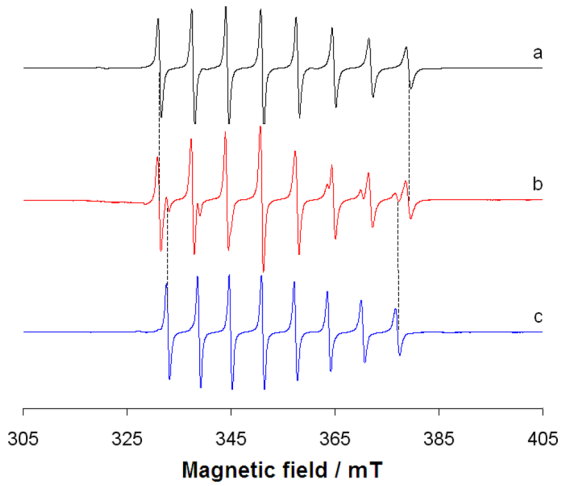

Figure 4. Room-temperature (298 K) EPR spectra recorded at pH 7.4 in aqueous solution in the systems containing (a) VDC/ox 1/10, (b) VDC/ox/$NaHCO_3$/lact/Na_2HPO_4 1/1/2706.5/164.1/119.6, and (c) VDC $NaHCO_3$ 1/10. The concentration of VDC was 4.0×10^{-4} M (b) or 1.0×10^{-3} M (a and c). With the dotted lines the resonances $M_I = -7/2, 7/2$ of the complexes $[Cp_2V(ox)]$ (trace a) and $[Cp_2V(CO_3)]$ (c) are shown.

$[Cp_2V(CO_3)]$ (Figure 4c) is formed only in a very small amount. Therefore, when the ratio VDC/ox is 1/1, almost all $[Cp_2V]^{2+}$ ion is bound by oxalate and the participation of the other bL is negligible. Analogous results are expected when the ratio VDC/ox is <1, i.e., when the concentration of VDC at physiological conditions is lower than 9.2 μM.

The behavior of the quinary system VDC/ox/$NaHCO_3$/lact/Na_2HPO_4 with ratio 1/0.1/270.7/16.4/12.0 is reported in Figure S13 of the Supporting Information, trace b. In such a system the main species is $[Cp_2V(CO_3)]$ (Figure S13, trace a), whereas two minor species are observable, $[Cp_2V(ox)]$ and probably $[Cp_2V(lactH_{-1})]$ (Figure S13, traces c and d). $[Cp_2V(HPO_4)]$, instead, is not formed. This behavior can be rationalized in the following way: when VDC is present in solution in excess with respect to oxalate (i.e., when it is present in the blood plasma with a concentration higher than 9.2 μM),

DOI: 10.1021/acs.inorgchem.5b01277
Inorg. Chem. 2015, 54, 8237−8250

the latter binds the maximum possible amount of $[Cp_2V]^{2+}$, whereas the remaining part of VDC distributes between the carbonate ion (mainly) and lactate (in much smaller concentration). The exact amount of the mixed complex with lactate cannot be determined because the resonances of $[Cp_2V(ox)]$ and $[Cp_2V(lactH_{-1})]$ fall in the same region of the EPR spectrum.

The electronic absorption spectra recorded in the two quinary systems VDC/ox/$NaHCO_3$/lact/Na_2HPO_4 with ratio 1/1/2706.5/164.1/119.6 and 1/0.1/270.7/16.4/12.0 (Figure 5) allowed us to confirm this finding. It can be noticed that in

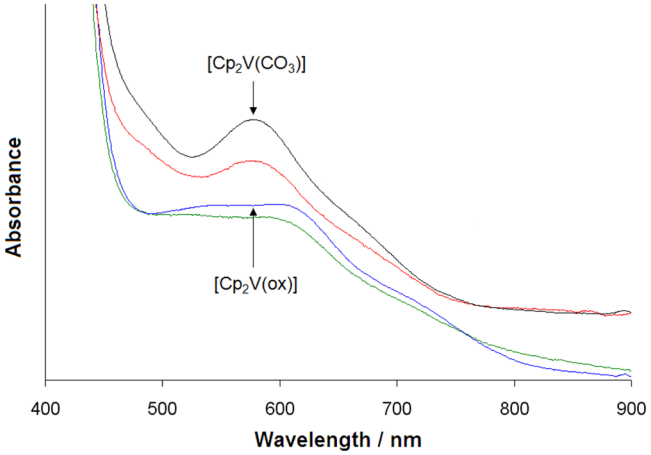

Figure 5. Electronic absorption spectra recorded in aqueous solution at pH 7.4 in the systems containing VDC/ox/$NaHCO_3$/lact/Na_2HPO_4 1/1/2706.5/164.1/119.6 (green), VDC/ox 1/10 (blue), VDC/ox/$NaHCO_3$/lact/Na_2HPO_4 1/0.1/270.7/16.4/12.0 (red), and VDC/$NaHCO_3$ 1/10 (black). VDC concentration was 4.0×10^{-4} (green and red) and 1.0×10^{-3} M (blue and black). Spectra of $[Cp_2V(CO_3)]$ and $[Cp_2V(ox)]$ are indicated by the two arrows.

the first case (VDC and oxalate at the equimolar ratio) the electronic absorption spectrum is comparable to that of $[Cp_2V(ox)]$ (in blue in Figure 5), whereas when an excess of VDC is present (for example, when it is 10 times more concentrated than oxalate) the spectrum closely resembles that of $[Cp_2V(CO_3)]$ (in black in Figure 5) with an absorption band at 575 nm.

The behavior at low temperature of the two systems VDC/ox/$NaHCO_3$/lact/Na_2HPO_4 at molar ratio 1/1/2706.5/164.1/119.6 and 1/0.1/270.7/16.4/12.0 is the same as described at room temperature. Frozen solutions EPR spectra are reported in Figures 6 and 7 and, as usual, are better resolved than the room-temperature ones. It can be observed that when the ratio VDC/ox is 1/1, the main species is $[Cp_2V(ox)]$, whereas $[Cp_2V(CO_3)]$ is the minor species; the spectrum recorded in the system with ratio 1/1/2706.5/164.1/119.6 can be reproduced postulating 70% of $[Cp_2V(ox)]$ and 30% of $[Cp_2V(CO_3)]$ in aqueous solution (Figure 6c). When the ratio VDC/ox is 10/1, instead, the main species is $[Cp_2V(CO_3)]$, whereas $[Cp_2V(ox)]$ and $[Cp_2V(lactH_{-1})]$ are the minor species; in this case the spectrum was simulated considering in aqueous solution 80% of $[Cp_2V(CO_3)]$, 10% of $[Cp_2V(ox)]$, and 10% of $[Cp_2V(lactH_{-1})]$ (Figure S14 of the Supporting Information).

5. Speciation of VDC in the Blood Plasma. After the investigation of the behavior of VDC in the blood model solutions, the speciation in the plasma was evaluated. To carry

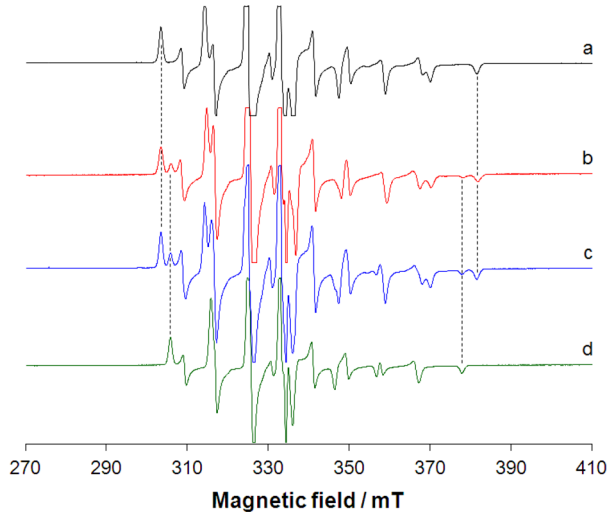

Figure 6. EPR spectra recorded at 120 K and pH 7.4 in aqueous solution in the systems containing (a) VDC/ox 1/10, (b) VDC/ox/$NaHCO_3$/lact/Na_2HPO_4 1/1/2706.5/164.1/119.6, (c) spectrum obtained in aqueous solution 70% of $[Cp_2V(ox)]$ (trace a) and 30% of $[Cp_2V(CO_3)]$ (trace d) and (d) VDC/$NaHCO_3$ 1/10. The concentration of VDC was 4.0×10^{-4} (b) and 1.0×10^{-3} M (a and c). With the dotted lines the resonances $M_I = -7/2, 7/2$ of the complexes $[Cp_2V(ox)]$ (a) and $[Cp_2V(CO_3)]$ (d) are shown.

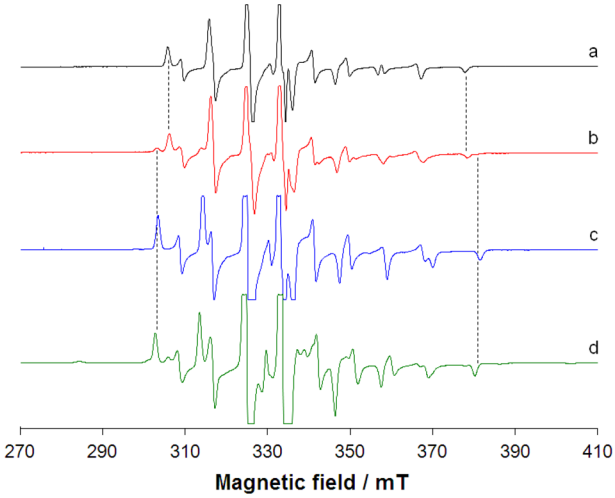

Figure 7. EPR spectra recorded at 120 K in aqueous solution at pH 7.4 in the systems containing (a) VDC/$NaHCO_3$ 1/10, (b) VDC/ox/$NaHCO_3$/lact/Na_2HPO_4 1/0.1/270.7/16.4/12.0, (c) VDC/ox 1/10, and (d) VDC/lact 1/10. The concentration of VDC was 4.0×10^{-4} M (b) and 1.0×10^{-3} M (a, c, and d). With the dotted lines the resonances $M_I = -7/2, 7/2$ of the complexes $[Cp_2V(CO_3)]$ (a), $[Cp_2V(ox)]$ (c), and $[Cp_2V(lactH_{-1})]$ (d) are shown.

out these experiments, a blood sample was centrifuged to separate plasma from buffy coat and red blood cells (see Experimental and Computational Section). The plasma was subsequently incubated for 30 min at 37 °C with a solution of VDC with a concentration of 4.5×10^{-5} M, and the EPR spectrum at 120 K was immediately measured. As pointed out in the literature,[37b] the analysis of a frozen solution EPR spectrum is preferred to that of room-temperature one because it allows one to get more detailed information on (i) the type of V(IV) species (nonoxido or oxido), (ii) the coordination mode, geometry, and distortion of V(IV) species, since the values of A_i

DOI: 10.1021/acs.inorgchem.5b01277
Inorg. Chem. 2015, 54, 8237−8250

(i = *x*, *y*, *z*) are more sensitive to the identity of the donors than A_{iso}, and (iii) the presence of minor species in solution, which usually are not detectable from the examination of a room-temperature spectrum. The EPR spectrum recorded in the blood plasma is shown in Figure 8a, together with the spectra of

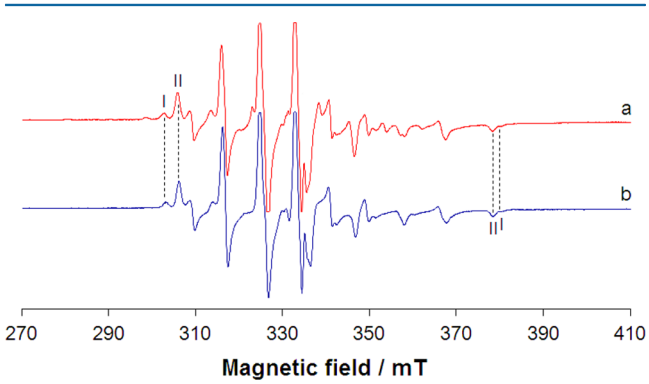

Figure 8. EPR spectra recorded at 120 K at pH 7.4 in the systems containing (a) blood plasma incubated with VDC for 30 min and (b) VDC/ox/$NaHCO_3$/lact/Na_2HPO_4 1/0.1/270.7/16.4/12.0. The concentration of VDC was 4.5×10^{-5} M (a) and 4.0×10^{-4} M (b). With the dotted lines the resonances $M_I = -7/2, 7/2$ of the complexes $[Cp_2V(ox)]$ (**I**) and $[Cp_2V(CO_3)]$ (**II**) are indicated.

the system VDC/ox/$NaHCO_3$/lact/Na_2HPO_4 at ratio 1/0.1/270.7/16.4/12.0 (Figure 8b). The results are very surprising: the behavior revealed in the blood plasma is perfectly superimposable to that observed in the model system, demonstrating that the study of a good model can give valuable information on the behavior of a more complicated system such as a biological one. From an examination of Figure 8, it can be observed that V(IV) distributes between oxalate and carbonate ion: in particular, the strongest ligand, oxalate (9.2 μM), binds 9.2 μM of VDC to form $[Cp_2V(ox)]$, whereas the remaining part of $[Cp_2V]^{2+}$ (35.8 μM) is complexed by carbonate as $[Cp_2V(CO_3)]$. The predicted ratio between the amounts of $[Cp_2V(CO_3)]$ and $[Cp_2V(ox)]$ should be ca. 4:1, in very good agreement with what was observed in the spectrum reported in Figure 8a.

Some years ago, Vinklárek and co-workers dissolved VDC in the blood plasma and recorded room-temperature EPR spectra; they found two sets of isotropic signals attributed to $[Cp_2V(CO_3)]$ and an unspecified species with an amino acid, $[Cp_2V(a.a.)]$.[45] The results of this study indicate that their results are partially correct: whereas $[Cp_2V(CO_3)]$ is—without any doubt—formed, the other species was confused with $[Cp_2V(a.a.)]$ (not formed) because its spectrum is characterized by an A_{iso} value similar to that of $[Cp_2V(ox)]$.

On the basis of the results discussed in this study, the speciation of $[Cp_2VCl_2]$ in the blood plasma can be illustrated in Scheme 4. After the oral administration VDC passes in solution at the acid pH of the stomach (where the two Cl^- ions are probably replaced by two H_2O ligands). When $[Cp_2V(H_2O)_2]^{2+}$ arrives in the small intestine and then in the bloodstream at pH 7.4, $[Cp_2V(OH)_2]$ is formed and can react with the bioligands of the plasma (in particular, oxalate, carbonate, and lactate, see above). The concentration of VDC in the plasma does not correspond to the administered dose; in fact, usually only 1−10% of orally ingested V compound is absorbed in the gastrointestinal tract, the real percent amount being influenced by several factors such as the chemical form

Scheme 4. Speciation of VDC in the Blood Plasma as a Function of Its Concentration[a]

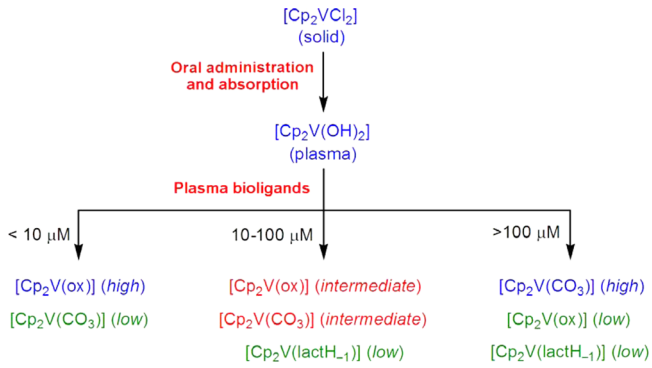

[a]With high, intermediate, and low the relative amount of each species is shown.

(inorganic salt or complex), the charge, and the polarity of the species.[61] A total concentration in the range 10−100 μM is plausible for an orally administered active V compound,[1b,60] the exact value depending mainly on the gastrointestinal tract absorption. If V concentration is around 10 μM, most of VDC administered is transported to the target organs in the organism as $[Cp_2V(ox)]$, i.e., the moiety $[Cp_2V]^{2+}$ is bound by the strongest bL bioligand, oxalate. If V concentration is 10 times higher, 100 μM, only 9.2 μM of $[Cp_2V]^{2+}$ is complexed by oxalate, whereas the remaining part distributes between carbonate which forms the main species $[Cp_2V(CO_3)]$ and lactate which forms the minor species $[Cp_2V(lactH_{-1})]$. When V concentration is in the intermediate concentration range, 10−100 μM, $[Cp_2V]^{2+}$ distributes between oxalate and carbonate, with the role of the latter being more important with increasing concentration with respect to the lowest limit of 10 μM.

CONCLUSIONS

It is now demonstrated that many vanadium compounds have antitumor activity. $[Cp_2VCl_2]$ or VDC has been the first V species with anticancer activity and has been proposed in 1983 in the treatment of Ehrlich ascites tumor. All VDC derivatives studied subsequently induce apoptosis in human cancer cells, but their mode of action remains elusive. The mechanism of VDC is closely related to the biotransformation in the blood plasma because the latter determines which species arrives to the target cells in the organism.

Therefore, in this study the speciation of VDC in the plasma under physiological conditions was studied. The results indicate that in an aqueous solution the two Cp−V bonds are very resistant to the hydrolysis, whereas both Cl^- ions dissociate to form at acid pH of the stomach $[Cp_2V(H_2O)_2]^{2+}$, which at physiological pH deprotonates quantitatively to $[Cp_2V(OH)_2]$. In contrast with what was found for other pharmacologically active V compounds, such as antidiabetic $V(IV)O^{2+}$ species, $[Cp_2V(OH)_2]$ does not interact with the plasma proteins (transferrin and albumin) and undergoes displacement reactions with the low molecular mass bioligands. The bioligands with highest affinity for $[Cp_2V]^{2+}$ moiety are oxalate, carbonate, lactate, and hydrogen phosphate, whereas other candidates to V binding such as citrate and amino acids do not show any affinity for it. On the basis of EPR, UV−vis, ESI-MS, MS-MS, and DFT results, it has been found that the affinity

DOI: 10.1021/acs.inorgchem.5b01277
Inorg. Chem. 2015, 54, 8237−8250

order of the four strongest bioligands is $ox^{2-} \gg CO_3^{2-} > lactH_{-1}^{2-} > HPO_4^{2-}$. The speciation of VDC at the physiological conditions has been examined studying several model systems containing the bioligands with the same relative amount as in the blood and, subsequently, carrying out experiments with plasma samples. The results obtained show that the model systems behave in the same way as the blood plasma, demonstrating that the choice of a good model is essential to get information on more complicated systems, such as the biological ones.

The speciation of VDC in the blood plasma can be summarized as follows: if V concentration is low (10 μM), most of VDC administered is transported in the organism as $[Cp_2V(ox)]$, i.e., the strongest bioligand, oxalate, binds the $[Cp_2V]^{2+}$ moiety. In contrast, if V concentration is high (100 μM) oxalate binds only 9.2 μM of $[Cp_2V]^{2+}$ (9.2 μM is the oxalate concentration in the plasma), whereas the remaining 90.8 μM of $[Cp_2V]^{2+}$ distributes between carbonate to form $[Cp_2V(CO_3)]$ (main species) and lactate to yield $[Cp_2V(lactH_{-1})]$ (minor species). Finally, if V concentration is in the range 10−100 μM, $[Cp_2V]^{2+}$ distributes between $[Cp_2V(ox)]$ and $[Cp_2V(CO_3)]$, with the role of carbonate being more and more important with increasing V concentration with respect to 10 μM.

■ ASSOCIATED CONTENT

Supporting Information

The Supporting Information is available free of charge on the ACS Publications website at DOI: 10.1021/acs.inorgchem.5b01277.

Tables and figures with the results of DFT calculations, figures with EPR spectra recorded at 298 and 120 K and pH 7.4 on VDC and its binary, ternary, quaternary and quinary systems, figure with electronic absorption spectra recorded at pH 7.4 on VDC and its binary systems, calculated and experimental isotopic pattern for the most intense peaks detected in the mass spectra (PDF)

■ AUTHOR INFORMATION

Corresponding Author

*E-mail: garribba@uniss.it.

Notes

The authors declare no competing financial interest.

■ ACKNOWLEDGMENTS

The authors thank Fondazione Banco di Sardegna for financial support (project Prot. U924.2014/AI.807.MGB; Prat. 2014.0443) and Servizio Trasfusionale Aziendale (ASL of Sassari).

■ REFERENCES

(1) (a) Crans, D. C.; Smee, J. J.; Gaidamauskas, E.; Yang, L. *Chem. Rev.* **2004**, *104*, 849−902. (b) Rehder, D. *Bioinorganic Vanadium Chemistry*; John Wiley & Sons, Ltd.: Chichester, 2008.

(2) (a) Thompson, K. H.; Orvig, C. *Coord. Chem. Rev.* **2001**, *219*−*221*, 1033−1053. (b) Shechter, Y.; Goldwaser, I.; Mironchik, M.; Fridkin, M.; Gefel, D. *Coord. Chem. Rev.* **2003**, *237*, 3−11. (c) Sakurai, H.; Yoshikawa, Y.; Yasui, H. *Chem. Soc. Rev.* **2008**, *37*, 2383−2392.

(3) (a) Thompson, K. H.; McNeill, J. H.; Orvig, C. *Chem. Rev.* **1999**, *99*, 2561−2572. (b) Thompson, K. H.; Orvig, C. In *Metal Ions in Biological Systems*; Sigel, H., Sigel, A., Eds.; Marcel Dekker: New York, 2004; Vol. *41*, pp 221−252. (c) Thompson, K. H.; Liboiron, B. D.; Hanson, G. R.; Orvig, C. In *Medicinal Inorganic Chemistry*; American Chemical Society: Washington, DC, 2005; Vol. *903*, pp 384−399. (d) Thompson, K. H.; Orvig, C. *J. Inorg. Biochem.* **2006**, *100*, 1925−1935.

(4) Thompson, K. H.; Lichter, J.; LeBel, C.; Scaife, M. C.; McNeill, J. H.; Orvig, C. *J. Inorg. Biochem.* **2009**, *103*, 554−558.

(5) Costa Pessoa, J.; Tomaz, I. *Curr. Med. Chem.* **2010**, *17*, 3701−3738.

(6) Carroll, J. http://www.fiercebiotech.com/story/akesis-shutters-program-files-chap-7/2009-01-22.

(7) (a) Rehder, D. *Future Med. Chem.* **2012**, *4*, 1823−1837. (b) Costa Pessoa, J.; Etcheverry, S.; Gambino, D. *Coord. Chem. Rev.* **2015**, 10.1016/j.ccr.2014.12.002.

(8) (a) Köpf-Maier, P.; Krahl, D. *Chem.-Biol. Interact.* **1983**, *44*, 317−328. (b) Köpf-Maier, P.; Köpf, H. *Chem. Rev.* **1987**, *87*, 1137−1152.

(9) (a) Ghosh, P.; D'Cruz, O. J.; Narla, R. K.; Uckun, F. M. *Clin. Cancer Res.* **2000**, *6*, 1536−1545. (b) Navara, C. S.; Benyumov, A.; Vassilev, A.; Narla, R. K.; Ghosh, P.; Uckun, F. M. *Anti-Cancer Drugs* **2001**, *12*, 369−376.

(10) (a) Lümmen, G.; Sperling, H.; Luboldt, H.; Otto, T.; Rübben, H. *Cancer Chemother. Pharmacol.* **1998**, *42*, 415−417. (b) Kröger, N.; Kleeberg, U. R.; Mross, K.; Edler, L.; Hossfeld, D. K. *Onkologie* **2000**, *23*, 60−62.

(11) Gleeson, B.; Claffey, J.; Hogan, M.; Müller-Bunz, H.; Wallis, D.; Tacke, M. *J. Organomet. Chem.* **2009**, *694*, 1369−1374.

(12) Gleeson, B.; Deally, A.; Müller-Bunz, H.; Patil, S.; Tacke, M. *Aust. J. Chem.* **2010**, *63*, 1514−1520.

(13) Honzíček, J.; Klepalová, I.; Vinklárek, J.; Padělková, Z.; Císařová, I.; Šiman, P.; Řezáčová, M. *Inorg. Chim. Acta* **2011**, *373*, 1−7.

(14) Yoshikawa, Y.; Sakurai, H.; Crans, D. C.; Micera, G.; Garribba, E. *Dalton Trans.* **2014**, *43*, 6965−6972.

(15) (a) Sanna, D.; Serra, M.; Micera, G.; Garribba, E. *Inorg. Chem.* **2014**, *53*, 1449−1464. (b) Sanna, D.; Serra, M.; Micera, G.; Garribba, E. *Inorg. Chim. Acta* **2014**, *420*, 75−84. (c) Sanna, D.; Fabbri, D.; Serra, M.; Buglyó, P.; Bíró, L.; Ugone, V.; Micera, G.; Garribba, E. *J. Inorg. Biochem.* **2015**, *147*, 71−84. (d) Levina, A.; McLeod, A. I.; Pulte, A.; Aitken, J. B.; Lay, P. A. *Inorg. Chem.* **2015**, *54*, 6707−6718. (e) Levina, A.; McLeod, A. I.; Gasparini, S. J.; Nguyen, A.; De Silva, W. G. M.; Aitken, J. B.; Harris, H. H.; Glover, C.; Johannessen, B.; Lay, P. A. *Inorg. Chem.* **2015**, *54*, 7753−7766.

(16) (a) Sanna, D.; Micera, G.; Garribba, E. *Inorg. Chem.* **2009**, *48*, 5747−5757. (b) Sanna, D.; Micera, G.; Garribba, E. *Inorg. Chem.* **2010**, *49*, 174−187. (c) Sanna, D.; Buglyó, P.; Micera, G.; Garribba, E. *JBIC, J. Biol. Inorg. Chem.* **2010**, *15*, 825−839. (d) Sanna, D.; Micera, G.; Garribba, E. *Inorg. Chem.* **2011**, *50*, 3717−3728. (e) Sanna, D.; Biro, L.; Buglyo, P.; Micera, G.; Garribba, E. *Metallomics* **2012**, *4*, 33−36. (f) Sanna, D.; Ugone, V.; Micera, G.; Garribba, E. *Dalton Trans.* **2012**, *41*, 7304−7318. (g) Sanna, D.; Bíró, L.; Buglyó, P.; Micera, G.; Garribba, E. *J. Inorg. Biochem.* **2012**, *115*, 87−99. (h) Sanna, D.; Micera, G.; Garribba, E. *Inorg. Chem.* **2013**, *52*, 11975−11985. (i) Koleša-Dobravc, T.; Lodyga-Chruscinska, E.; Symonowicz, M.; Sanna, D.; Meden, A.; Perdih, F.; Garribba, E. *Inorg. Chem.* **2014**, *53*, 7960−7976.

(17) (a) Willsky, G. R.; Goldfine, A. B.; Kostyniak, P. J.; McNeill, J. H.; Yang, L. Q.; Khan, H. R.; Crans, D. C. *J. Inorg. Biochem.* **2001**, *85*, 33−42. (b) Liboiron, B. D.; Thompson, K. H.; Hanson, G. R.; Lam, E.; Aebischer, N.; Orvig, C. *J. Am. Chem. Soc.* **2005**, *127*, 5104−5115. (c) Jakusch, T.; Costa Pessoa, J.; Kiss, T. *Coord. Chem. Rev.* **2011**, *255*, 2218−2226. (d) Correia, I.; Jakusch, T.; Cobbinna, E.; Mehtab, S.; Tomaz, I.; Nagy, N. V.; Rockenbauer, A.; Costa Pessoa, J.; Kiss, T. *Dalton Trans.* **2012**, *41*, 6477−6487. (e) Vincent, J. B.; Love, S. *Biochim. Biophys. Acta, Gen. Subj.* **2012**, *1820*, 362−378. (f) Mehtab, S.; Gonçalves, G.; Roy, S.; Tomaz, A. I.; Santos-Silva, T.; Santos, M. F. A.; Romão, M. J.; Jakusch, T.; Kiss, T.; Costa Pessoa, J. *J. Inorg. Biochem.* **2013**, *121*, 187−195. (g) Gonçalves, G.; Tomaz, A. I.; Correia, I.; Veiros, L. F.; Castro, M. M. C. A.; Avecilla, F.; Palacio, L.; Maestro, M.; Kiss, T.; Jakusch, T.; Garcia, M. H. V.; Costa Pessoa, J. *Dalton Trans.* **2013**, *42*, 11841−11861. (h) Costa Pessoa, J.; Garribba, E.; Santos, M. F. A.; Santos-Silva, T. *Coord. Chem. Rev.* **2015**, DOI: 10.1016/j.ccr.2015.03.016.

DOI: 10.1021/acs.inorgchem.5b01277
Inorg. Chem. 2015, 54, 8237−8250

(18) Santos, M. F. A.; Correia, I.; Oliveira, A. R.; Garribba, E.; Costa Pessoa, J.; Santos-Silva, T. *Eur. J. Inorg. Chem.* **2014**, 3293−3297.
(19) Harris, W. R. *Clin. Chem.* **1992**, *38*, 1809−1818.
(20) Kiss, T.; Kiss, E.; Garribba, E.; Sakurai, H. *J. Inorg. Biochem.* **2000**, *80*, 65−73.
(21) Gómez-Ruiz, S.; Maksimović-Ivanić, D.; Mijatović, S.; Kaluđerović, G. N. *Bioinorg. Chem. Appl.* **2012**, 140248.
(22) Garner, C. D.; Collison, D.; Mabbs, F. E. In *Vanadium and its role in life*, Sigel, H., Sigel, A., Eds.; Marcel Dekker, Inc.: New York, 1995; Vol. *31*, pp 617−670.
(23) (a) Morgenstern, B.; Steinhauser, S.; Hegetschweiler, K.; Garribba, E.; Micera, G.; Sanna, D.; Nagy, L. *Inorg. Chem.* **2004**, *43*, 3116−3126. (b) Rangel, M.; Leite, A.; Amorim, M. J.; Garribba, E.; Micera, G.; Lodyga-Chruscinska, E. *Inorg. Chem.* **2006**, *45*, 8086−8097. (c) Morgenstern, B.; Kutzky, B.; Neis, C.; Stucky, S.; Hegetschweiler, K.; Garribba, E.; Micera, G. *Inorg. Chem.* **2007**, *46*, 3903−3915.
(24) Micera, G.; Sanna, D. In *Vanadium in the environment Part I: Chemistry and Biochemistry*; Nriagu, J. O., Ed.; Wiley: New York, 1998; pp 131−166.
(25) Henderson, W.; McIndoe, J. S. *Mass Spectrometry of Inorganic, Coordination and Organometallic Compounds*; John Wiley & Sons, Ltd.: Chichester, 2005.
(26) (a) Doležel, P.; Kubáň, V. *Chem. Pap.* **2002**, *56*, 236−240. (b) Di Marco, V. B.; Bombi, G. G. *Mass Spectrom. Rev.* **2006**, *25*, 347−379. (c) Esteban-Fernandez, D.; Canas, B.; Pizarro, I.; Palacios, M. A.; Gomez-Gomez, M. M. *J. Anal. At. Spectrom.* **2007**, *22*, 1113−1121. (d) Sekar, R.; Kailasa, S. K.; Abdelhamid, H. N.; Chen, Y.-C.; Wu, H.-F. *Int. J. Mass Spectrom.* **2013**, *338*, 23−29. (e) Sgarbossa, P.; Sbovata, S. M.; Bertani, R.; Mozzon, M.; Benetollo, F.; Marzano, C.; Gandin, V.; Michelin, R. A. *Inorg. Chem.* **2013**, *52*, 5729−5741. (f) Telpoukhovskaia, M. A.; Rodríguez-Rodríguez, C.; Scott, L. E.; Page, B. D. G.; Patrick, B. O.; Orvig, C. *J. Inorg. Biochem.* **2014**, *132*, 59−66. (g) Pivetta, T.; Lallai, V.; Valletta, E.; Trudu, F.; Isaia, F.; Perra, D.; Pinna, E.; Pani, A. *J. Inorg. Biochem.* **2015**, DOI: 10.1016/j.jinorgbio.2015.05.004.
(27) (a) Sanna, D.; Pecoraro, V.; Micera, G.; Garribba, E. *JBIC, J. Biol. Inorg. Chem.* **2012**, *17*, 773−790. (b) Justino, G. C.; Garribba, E.; Costa Pessoa, J. *JBIC, J. Biol. Inorg. Chem.* **2013**, *18*, 803−813.
(28) Jakusch, T.; Hollender, D.; Enyedy, E. A.; Gonzalez, C. S.; Montes-Bayon, M.; Sanz-Medel, A.; Costa Pessoa, J.; Tomaz, I.; Kiss, T. *Dalton Trans.* **2009**, 2428−2437.
(29) Kiss, T.; Jakusch, T.; Gyurcsik, B.; Lakatos, A.; Enyedy, É. A.; Sija, É. *Coord. Chem. Rev.* **2012**, *256*, 125−132.
(30) Sanna, D.; Garribba, E.; Micera, G. *J. Inorg. Biochem.* **2009**, *103*, 648−655.
(31) (a) Strohalm, M.; Hassman, M.; Košata, B.; Kodíček, M. *Rapid Commun. Mass Spectrom.* **2008**, *22*, 905−908. (b) Strohalm, M.; Kavan, D.; Novák, P.; Volný, M.; Havlíček, V. *Anal. Chem.* **2010**, *82*, 4648−4651. (c) Niedermeyer, T. H. J.; Strohalm, M. *PLoS One* **2012**, *7*, e44913.
(32) Frisch, M. J.; Trucks, G. W.; Schlegel, H. B.; Scuseria, G. E.; Robb, M. A.; Cheeseman, J. R.; Montgomery, J. A., Jr.; Vreven, T.; Kudin, K. N.; Burant, J. C.; Millam, J. M.; Iyengar, S. S.; Tomasi, J.; Barone, V.; Mennucci, B.; Cossi, M.; Scalmani, G.; Rega, N.; Petersson, G. A.; Nakatsuji, H.; Hada, M.; Ehara, M.; Toyota, K.; Fukuda, R.; Hasegawa, J.; Ishida, M.; Nakajima, T.; Honda, Y.; Kitao, O.; Nakai, H.; Klene, M.; Li, X.; Knox, J. E.; Hratchian, H. P.; Cross, J. B.; Adamo, C.; Jaramillo, J.; Gomperts, R.; Stratmann, R. E.; Yazyev, O.; Austin, A. J.; Cammi, R.; Pomelli, C.; Ochterski, J. W.; Ayala, P. Y.; Morokuma, K.; Voth, G. A.; Salvador, P.; Dannenberg, J. J.; Zakrzewski, V. G.; Dapprich, S.; Daniels, A. D.; Strain, M. C.; Farkas, O.; Malick, D. K.; Rabuck, A. D.; Raghavachari, K.; Foresman, J. B.; Ortiz, J. V.; Cui, Q.; Baboul, A. G.; Clifford, S.; Cioslowski, J.; Stefanov, B. B.; Liu, G.; Liashenko, A.; Piskorz, P.; Komaromi, I.; Martin, R. L.; Fox, D. J.; Keith, T.; Al-Laham, M. A.; Peng, C. Y.; Nanayakkara, A.; Challacombe, M.; Gill, P. M. W.; Johnson, B.; Chen, W.; Wong, M. W.; Gonzalez, C.; Pople, J. A. *Gaussian 03*, revision C.02; Gaussian, Inc.: Wallingford, CT, 2004.
(33) (a) Neese, F. *Wiley Interdiscip. Rev. Comput. Mol. Sci.* **2012**, *2*, 73−78. (b) Neese, F. *ORCA-An Ab Initio, DFT and Semiempirical Program Package*, Version 3.0; Max-Planck-Institute for Chemical Energy Conversion: Mülheim a. d. Ruhr, 2013.
(34) Micera, G.; Garribba, E. *Int. J. Quantum Chem.* **2012**, *112*, 2486−2498.
(35) (a) Bühl, M.; Kabrede, H. *J. Chem. Theory Comput.* **2006**, *2*, 1282−1290. (b) Bühl, M.; Reimann, C.; Pantazis, D. A.; Bredow, T.; Neese, F. *J. Chem. Theory Comput.* **2008**, *4*, 1449−1459.
(36) (a) Micera, G.; Pecoraro, V. L.; Garribba, E. *Inorg. Chem.* **2009**, *48*, 5790−5796. (b) Micera, G.; Garribba, E. *Eur. J. Inorg. Chem.* **2010**, 4697−4710. (c) Micera, G.; Garribba, E. *Eur. J. Inorg. Chem.* **2011**, 3768−3780. (d) Sanna, D.; Varnágy, K.; Timári, S.; Micera, G.; Garribba, E. *Inorg. Chem.* **2011**, *50*, 10328−10341. (e) Sanna, D.; Buglyo, P.; Biro, L.; Micera, G.; Garribba, E. *Eur. J. Inorg. Chem.* **2012**, 1079−1092. (f) Sanna, D.; Buglyo, P.; Tomaz, A. I.; Costa Pessoa, J.; Borovic, S.; Micera, G.; Garribba, E. *Dalton Trans.* **2012**, *41*, 12824−12838. (g) Justino, G.; Garribba, E.; Costa Pessoa, J. *JBIC, J. Biol. Inorg. Chem.* **2013**, *18*, 803−813.
(37) (a) Micera, G.; Garribba, E. *Dalton Trans.* **2009**, 1914−1918. (b) Gorelsky, S.; Micera, G.; Garribba, E. *Chem. - Eur. J.* **2010**, *16*, 8167−8180. (c) Micera, G.; Garribba, E. *J. Comput. Chem.* **2011**, *32*, 2822−2835.
(38) (a) Tzavellas, N.; Klouras, N.; Raptopoulou, C. P. *Z. Anorg. Allg. Chem.* **1996**, *622*, 898−902. (b) Honzíček, J.; Vinklárek, J.; Císařová, I.; Erben, M. *Inorg. Chim. Acta* **2009**, *362*, 83−88.
(39) Toney, J. H.; Brock, C. P.; Marks, T. J. *J. Am. Chem. Soc.* **1986**, *108*, 7263−7274.
(40) Toney, J. H.; Marks, T. J. *J. Am. Chem. Soc.* **1985**, *107*, 947−953.
(41) Pavlik, I.; Vinklárek, J. *Eur. J. Solid State Inorg. Chem.* **1991**, *28*, 815−827.
(42) (a) Munzarová, M. L. In *Calculation of NMR and EPR Parameters*; Kaupp, M., Bühl, M., Malkin, V. G., Eds.; Wiley-VCH Verlag GmbH & Co. KGaA: Weinheim, 2004; pp 461−482. (b) Neese, F. *Coord. Chem. Rev.* **2009**, *253*, 526−563.
(43) (a) Munzarová, M. L.; Kaupp, M. *J. Phys. Chem. B* **2001**, *105*, 12644−12652. (b) Neese, F. *J. Chem. Phys.* **2003**, *118*, 3939−3948. (c) Saladino, A. C.; Larsen, S. C. *J. Phys. Chem. A* **2003**, *107*, 1872−1878. (d) Aznar, C. P.; Deligiannakis, Y.; Tolis, E. J.; Kabanos, T.; Brynda, M.; Britt, R. D. *J. Phys. Chem. A* **2004**, *108*, 4310−4321. (e) Saladino, A. C.; Larsen, S. C. *Catal. Today* **2005**, *105*, 122−133. (f) King, A. E.; Nippe, M.; Atanasov, M.; Chantarojsiri, T.; Wray, C. A.; Bill, E.; Neese, F.; Long, J. R.; Chang, C. J. *Inorg. Chem.* **2014**, *53*, 11388−11395.
(44) (a) Pisano, L.; Varnagy, K.; Timari, S.; Hegetschweiler, K.; Micera, G.; Garribba, E. *Inorg. Chem.* **2013**, *52*, 5260−5272. (b) Sanna, D.; Varnagy, K.; Lihi, N.; Micera, G.; Garribba, E. *Inorg. Chem.* **2013**, *52*, 8202−8213. (c) Lodyga-Chruscinska, E.; Szebeszczyk, A.; Sanna, D.; Hegetschweiler, K.; Micera, G.; Garribba, E. *Dalton Trans.* **2013**, *42*, 13404−13416.
(45) Vinklárek, J.; Paláčková, H.; Honzíček, J.; Holubová, J.; Holčapek, M.; Císařová, I. *Inorg. Chem.* **2006**, *45*, 2156−2162.
(46) (a) Vinklárek, J.; Dědourková, T.; Honzíček, J.; Růžička, A. *J. Inorg. Biochem.* **2010**, *104*, 936−943. (b) Vinklárek, J.; Honzíček, J.; Erben, M.; Klepalová, I.; Eisner, A.; Růžička, A. *Inorg. Chim. Acta* **2013**, *405*, 121−127.
(47) Vinklárek, J.; Honzíček, J.; Holubová, J. *Inorg. Chim. Acta* **2004**, *357*, 3765−3769.
(48) Honzíček, J.; Nachtigall, P.; Císařová, I.; Vinklárek, J. *J. Organomet. Chem.* **2004**, *689*, 1180−1187.
(49) Vinklárek, J.; Honzíček, J.; Holubová, J. *Magn. Reson. Chem.* **2004**, *42*, 870−874.
(50) (a) Micera, G.; Sanna, D.; Dessì, A.; Kiss, T.; Buglyó, P. *Gazz. Chim. Ital.* **1993**, *123*, 573−577. (b) Garribba, E.; Micera, G.; Panzanelli, A.; Sanna, D. *Inorg. Chem.* **2003**, *42*, 3981−3987.
(51) Bakhtiar, R.; Tse, F. L. S. *Mutagenesis* **2000**, *15*, 415−430.
(52) Lodyga-Chruscinska, E.; Sanna, D.; Garribba, E.; Micera, G. *Dalton Trans.* **2008**, 4903−4916.

DOI: 10.1021/acs.inorgchem.5b01277
Inorg. Chem. 2015, 54, 8237−8250

(53) Du, H.; Xiang, J.; Zhang, Y.; Tang, Y.; Xu, G. *J. Inorg. Biochem.* **2008**, *102*, 146−149.
(54) Nishida, Y.; Niinuma, A.; Abe, K. *Inorg. Chem. Commun.* **2009**, *12*, 198−200.
(55) Kiss, T.; Jakusch, T.; Bouhsina, S.; Sakurai, H.; Enyedy, É. A. *Eur. J. Inorg. Chem.* **2006**, 3607−3613.
(56) Guo, M.; Sun, H.; McArdle, H. J.; Gambling, L.; Sadler, P. J. *Biochemistry* **2000**, *39*, 10023−10033.
(57) Chasteen, D. N. *Coord. Chem. Rev.* **1977**, *22*, 1−36.
(58) White, L. K.; Chasteen, N. D. *J. Phys. Chem.* **1979**, *83*, 279−284.
(59) Tinoco, A. D.; Eames, E. V.; Valentine, A. M. *J. Am. Chem. Soc.* **2008**, *130*, 2262−2270.
(60) (a) Thompson, K. H.; Battell, M.; McNeill, J. H. In *Vanadium in the Environment, Part 2: Health Effects: Toxycology of Vanadium in Mammals*; Nriagu, J. O., Ed.; Wiley: New York, 1998; pp 21−37. (b) Rehder, D.; Costa Pessoa, J.; Geraldes, C.; Castro, M.; Kabanos, T.; Kiss, T.; Meier, B.; Micera, G.; Pettersson, L.; Rangel, M.; Salifoglou, A.; Turel, I.; Wang, D. *JBIC, J. Biol. Inorg. Chem.* **2002**, *7*, 384−396. (c) Sakurai, H.; Fugono, J.; Yasui, H. *Mini-Rev. Med. Chem.* **2004**, *4*, 41−48. (d) Zhang, S.-Q.; Zhong, X.-Y.; Chen, G.-H.; Lu, W.-L.; Zhang, Q. *J. Pharm. Pharmacol.* **2008**, *60*, 99−105.
(61) (a) Nielsen, F. H. In *Metal ions in biological systems*; Sigel, H., Sigel, A., Eds.; Marcel Dekker: New York, 1995; Vol. *31*, pp 543−573. (b) Nielsen, F. H. In *Vanadium Compounds. Chemistry, Biochemistry, and Therapeutic Applications*; American Chemical Society: Washington DC, 1998; Vol. *711*, pp 297−307.

DOI: 10.1021/acs.inorgchem.5b01277
Inorg. Chem. 2015, 54, 8237−8250